Chapter 5
Hydrogen

5.1 Introduction

Hydrogen energy is a clean or inexhaustible energy like renewable energy and nuclear energy.

Today's energy supply has a considerable impact on the environment. Hydrogen energy is a promising alternative solution because it is clean and environmentally safe. It also produces negligible levels of greenhouse gases and other pollutants when compared with the fossil energy sources they replace. It is well-known that hydrogen is a clean and renewable fuel. Hydrogen is a secondary source of energy—an energy carrier—which is used to move, store and deliver energy in an easily usable form.

Future energy technology will utilize hydrogen with an increasing trend in steady as well as unsteady combustion processes. Hydrogen is the most common element in the universe and can be made from water. Converting hydrogen into energy is compatible with existing energy technologies, such as fuel cells, engines, and combustion turbines.

Hydrogen is produced from fossil fuels, hydrocarbon polymers, biomass, and water by electrolysis, and the biological processes of photolysis or thermolysis. Hydrogen gas may be stored as a gas or as a liquid. Hydrogen possesses properties that make it an ideal fuel for internal combustion engines. Hydrogen could be used advantageously as a clean energy carrier for heat supply and transportation purposes. However, the very high cost of hydrogen fuel and hydrogen vehicles is thought to outweigh the environmental advantages. It serves as an agent, through which a primary energy source (nuclear, solar, etc.) can be stored, transmitted and utilized to fulfill present and future energy needs. In the future, hydrogen may be used in furnaces and as a transportation fuel for automobiles, buses, trains, ships and airplanes. Hydrogen could also be converted directly into electricity by fuel cells (Caglar and Ozmen, 2000). Fuel cells can produce electricity and heat from hydrogen, natural gas, and petroleum fuels, and fuel gases derived from coal and

biomass. What makes fuel cells unique is that they can use fuels without combustion, simply by chemical reactions, making them extremely clean and efficient.

Hydrogen is considered one of the most promising fuels for generalized use in the future, mainly because it is an energy-efficient, low-polluting and renewable fuel. Much of the hydrogen produced in the world, and especially for the petrochemical industry, is obtained from natural gas, which is mostly made up of methane. The following energy carriers methanol, dimethyl ether, ethanol, gasoline, diesel, and propane can be utilized for hydrogen production in a reformer with autothermal reforming, that is a partial oxidation reformer above a temperature of 825 K (Höhlein et al., 2000).

Hydrogen can be generated from renewable energy sources such as from biomass, hydropower, solar thermal energy, solar energy using photovoltaics for direct conversion, and wind power. In the future, hydrogen could also be produced by gasification of biomass (Miranda, 2004). The only primary hydrogen combustion product is water. There is no CO_2, no CO, no sulfuric acid, no soot, no unburned hydrocarbons, and only very small amounts of NO_x are produced (Koroneos et al., 2005). Because hydrogen can be easily generated from renewable energy sources and water it has great potential as an energy source. However, storage of hydrogen in liquid form is difficult, as very low temperatures are required to liquefy hydrogen (Demirbas, 2002).

5.2 History

In 1766, hydrogen was first identified as a distinct element by British scientist Henry Cavendish after he evolved hydrogen gas by reacting zinc metal with hydrochloric acid. In a demonstration to the Royal Society of London, Cavendish applied a spark to hydrogen gas yielding water. This discovery led to his later finding that water is made of hydrogen and oxygen. In 1788, building on the discoveries of Cavendish, French chemist Antoine Lavoisier gave hydrogen its name, which was derived from the Greek words *hydro* and *genes*, meaning *water* and *born of* or *forming*. In 1800, English scientists William Nicholson and Sir Anthony Carlisle discovered that applying electric current to water produced hydrogen and oxygen gases by electrolysis. In 1838 the fuel cell effect, combining hydrogen and oxygen gases to produce water and an electric current, was discovered by Swiss chemist Christian Friedrich Schoenbein. In 1889, Ludwig Mond and Charles Langer attempted to build the first fuel cell device using air and industrial coal gas. They named the device a fuel cell (Caglar and Ozmen, 2000).

In the 1920s, German engineer Rudolf Erren, converted the internal combustion engines of trucks, buses, and submarines to use hydrogen or hydrogen mixtures. British scientist and Marxist writer, J.B.S. Haldane, introduced the concept of renewable hydrogen in his paper "Science and the Future" by proposing that "there will be great power stations where during windy weather the surplus power will be used for the electrolytic decomposition of water into oxygen and hydrogen."

In 1958, The United States formed the National Aeronautics and Space Administration (NASA). NASA's space program currently uses the most liquid hydrogen worldwide, primarily for rocket propulsion and as a fuel for fuel cells. In 1959, Francis T. Bacon of Cambridge University in England built the first practical hydrogen-air fuel cell. The 5-kilowatt (kW) system powered a welding machine. In 1970, electrochemist John O'M. Bockris coined the term "hydrogen economy" during a discussion at the General Motors (GM) Technical Center in Warren, Michigan. In 1973, after the OPEC oil embargo and the resulting supply shock suggested that the era of cheap petroleum had ended and that the world needed alternative fuels, the development of hydrogen fuel cells for conventional commercial applications began. In 1974, the National Science Foundation transferred the Federal Hydrogen R&D Program to the US Department of Energy. Professor T. Nejat Veziroglu of the University of Miami organized The Hydrogen Economy Miami Energy Conference (THEME), the first international conference held to discuss hydrogen energy. In 1990, the world's first solar-powered hydrogen production plant at Solar-Wasserstoff-Bayern, a research and testing facility in southern Germany, became operational. In 1994, Daimler Benz demonstrated its first NECAR I (New Electric CAR) fuel cell vehicle at a press conference in Ulm, Germany. In 2000, Ballard Power Systems presented the world's first production-ready PEM fuel cell for automotive applications at the Detroit Auto Show. In 2004, the world's first fuel cell-powered submarine underwent deepwater trials (Caglar and Ozmen, 2000).

5.3 Properties of Hydrogen

Hydrogen is a colorless, tasteless gas and it is the lightest chemical substance. The hydrogen molecule is non-polar; the weak nature of the intermolecular forces of attraction is indicated by the low normal boiling point (15.5 K), the normal melting point (14.1 K) and the critical temperature (30.2 K at a critical pressure of 12.8 atm). Hydrogen is virtually insoluble in water; approximately 2 ml of hydrogen will dissolve in 1l of water at room temperature and atmospheric pressure. There are three isotopes of hydrogen. The most abundant isotope ${}_1H^1$, constitutes 99.985% of naturally occurring hydrogen; deuterium ${}_1H^2$ (also indicated as ${}_1D^2$), constitutes 0.015%; and the radioactive tritium ${}_1H^3$ (also indicated as ${}_1T^3$) occurs only in trace amounts.

Hydrogen consists of a mixture of two types of molecules, *ortho*-hydrogen, in which the two proton spins are parallel, and *para*-hydrogen, in which they are antiparallel. There are a number of possible methods of measuring the proportion of *ortho*- to *para*-molecules in a sample of hydrogen gas (Farkas, 1935; Stewart and Squires, 1955; Noganow, 1992; Silvera and Pravica, 1998). Figure 5.1 shows the schematic model of the *ortho*/*para*-H_2 conversion on solid surfaces (Buntkowsky et al., 2006).

Figure 5.2 shows the structure of the hydrogen molecule. Two hydrogen atoms, each with one electron, combine to form a hydrogen molecule, in which the two

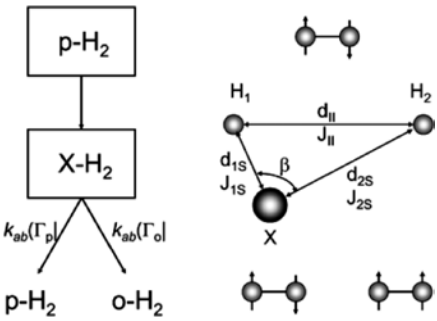

Fig. 5.1 Schematic model of the *ortho*/*para*-H_2 conversion on solid surfaces

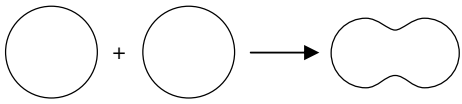

Fig. 5.2 Structure of the hydrogen molecule

electrons are shared between the atoms and serve to give each atom a filled valence shell. The simplest chemical bond is that formed between two hydrogen atoms. Each hydrogen atom has one electron. As the two atoms approach each other, the nucleus of one atom attracts the electron of the other. Eventually the two orbitals overlap, becoming a single orbital containing two electrons.

5.4 Fuel Properties of Hydrogen

Hydrogen is a synthetic energy carrier. It carries energy generated by some other process. The combustion products of hydrogen when it is burned completely with air consist of water, oxygen, and nitrogen—although it has been suggested that hydrogen is too valuable to burn. Laboratory tests conducted on internal combustion engines burning hydrogen demonstrate good performance (Berry et al., 1996). In comparison with an engine burning gasoline, the emission of nitrogen oxides is far less for the engine fueled by hydrogen. The product of hydrogen combustion with air is water vapor and negligible pollution when the peak temperature is limited. Some oxides of nitrogen (NO_x) are formed at very high combustion temperatures (< 2300 K); fortunately, the autoignition temperature of hydrogen is only 858 K.

Hydrogen is emerging as the favorite alternative to fossil fuels as an energy carrier, since it has good properties as a motor fuel and it can be used in internal combustion engines of automobiles. Some of the characteristic properties of a hydrogen-air mixture that can definitely influence the engine design and performance

are low ignition energy, low density, a wide range of ignition limits, high diffusion speed, and high flame speed (Plass et al., 1990).

The bond energy of the H-H bond is 431 kJ/mol. Electron affinity of hydrogen is low (–72 kJ/mol), where hydrogen reacts in this manner only with the most reactive metals. The ionization potential of hydrogen is relatively high (1312 kJ/mol). Hydrogen burns with a very hot flame and explosion in air:

$$2H_2+O_2 \rightarrow 2H_2O + Q \tag{5.1}$$

The higher heating value (HHV) of hydrogen is $Q_{HHV} = 142.324$ kJ/kg or $Q_{HHV} = 284.648$ kJ/kg mol. The lower heating value (LHV) of hydrogen is $Q_{LHV} = 118.976$ kJ/kg mol.

The catch fire energy of hydrogen is the lowest compared to other fuels. While the ignition energy of a gasoline-air mixture is 0.2 and 0.4 MJ under atmospheric pressure and ambient temperature, it is about 0.02 MJ for hydrogen-air mixtures. The ignition barrier, as a percentage of hydrogen by volume in a hydrogen-air mixture, is found between the lowest limit of 4–10% and the highest limit of 60–75% (Caglar and Ozmen, 2000).

Hydrogen reacts with the reactive metals to produce metal hydrides:

$$2Na\ (s) + H_2\ (g) \rightarrow 2NaH \tag{5.2}$$

Hydrogen reacts with many metal oxides to produce water and the free metal:

$$CuO\ (s) + H_2\ (g) \rightarrow Cu\ (s) + H_2O\ (g) \tag{5.3}$$

$$WO_3\ (s) + 3H_2\ (g) \rightarrow W\ (s) + 3H_2O\ (g) \tag{5.4}$$

Some of these reactions are employed in the metallurgy of oxide ores, for example, in the commercial production of tungsten metal. WO_3 in Eq. 5.4 is reduced to the free metal by hydrogen.

CO and H_2 react at high temperatures in the presence of a catalyst to produce methanol:

$$CO\ (g) + 2H_2\ (g) \rightarrow CH_3OH\ (g) \tag{5.5}$$

Hydrogen reacts with nitrogen at high pressures (300 to 1000 atm) and at high temperatures (675 to 875 K), in the presence of a catalyst to produce ammonia:

$$3H_2\ (g) + N_2\ (g) \rightarrow 2NH_3\ (g) \tag{5.6}$$

The advantages of hydrogen as a universal energy medium are: (a) the combustion of hydrogen results in the formation of steam and liquid water; (b) it is nontoxic and, as an energy carrier, extremely environmentally benign since water is the only exhaust product when hydrogen is converted into energy; (c) it is possible to produce hydrogen from the most abundant chemical on earth: water; (d) hydrogen can be used as a feedstock for numerous chemicals; (e) it is the most suitable fuel for use in fuel cells; and (f) transmission of energy in the form of hydrogen is more economical than through high-voltage AC lines for large distances. Table 5.1 shows the fuel properties of hydrogen (Midilli et al., 2005).

Table 5.1 Fuel properties of hydrogen

Property	Unit	Value
Boiling point	K	20.41
Freezing point	K	13.97
Density (liquid)	kg/m³	70.8
Specific heat at constant pressure	kJ/kg K	14.89
Explosion limits in air	% (vol.)	4–75
Ignition energy in air	mJ (millijoule)	0.02
Ignition temperature	K	585
Flame temperature in air	K	2318
Flame emissivity	%	17–25
Stoichiometric mixture in air	%	29.53
Stoichiometric air/fuel	kg/kg	34.3/1
Flame velocity	cm/s	2.75
HHV and LHV	MJ/kg	141.9–119.90
HHV and LHV	MJ/m³	11.89–10.05

5.5 Hydrogen Production Processes

Today the two most common methods used to produce hydrogen are: (1) steam reforming of natural gas, and (2) electrolysis of water. The predominant method for producing synthesis gas is steam reforming of natural gas, although other hydrocarbons can be used as feedstocks. For example, hydrogen can be produced from the biomass reforming process.

Hydrogen is produced commercially in almost a dozen processes. Most of them involve the extraction of the "hydro" part from hydrocarbons. The most widely used, least costly process is steam reforming, in which natural gas is made to react with steam, releasing hydrogen (Hohhmann, 2002). While using steam to reform natural gas has proven the cheapest way to produce commercial hydrogen, natural gas is still a hydrocarbon and emits CO_2 in the conversion process (Rifkin, 2002; Arni, 2004). Global hydrogen is produced from natural gas, oil, coal, and water by electrolysis with percentages of 48, 30, 18, and 4%, respectively. The main hydrogen production processes are given in Table 5.2.

Table 5.2 Main hydrogen production processes

Method	Process	Feedstock
Thermal	Steam reformation	Natural gas
	Thermochemical water splitting	Water
	Pyrolysis	Biomass
	Gasification	Coal, biomass
Electrochemical	Electrolysis	Water
	Photoelectrochemical	Water
Biological	Photobiological	Water and algae
	Fermentative microorganisms	strains
	Anaerobic digestion	Biomass
		Biomass

5.5.1 Hydrogen from Natural Gas by Steam Reforming

Hydrogen can also be extracted or "reformed" from natural gas. The process of steam reforming of hydrocarbons, developed in 1924, is the main industrial method for production of hydrogen. In the steam reforming reaction, steam reacts with hydrocarbons in the feed to predominantly produce carbon monoxide and hydrogen, commonly called synthesis gas. Natural gas or methane reforming is widely used in industry to obtain hydrogen or syngas (H_2 + CO), which are utilized in industry.

Steam reforming of natural gas is currently the least expensive method of producing hydrogen, and used for about half of the world's production of hydrogen. Steam reforming of methane has been carried out at high temperatures (Rostrup-Nielsen, 1984). The steam reforming is a highly endothermic reaction of methane and steam whereas the partial oxidation is slightly exothermic:

$$CH_4 + H_2O \rightarrow CO + 3H_2 \qquad \Delta H^o = 206 \text{ kJ/mol} \tag{5.7}$$

$$CH_4 + 0.5O_2 \rightarrow CO + 2H_2 \qquad \Delta H^o = -36 \text{ kJ/mol} \tag{5.8}$$

CH_4 is a very stable molecule and has to be processed under very severe conditions. Although its conversion to synthesis gas can be conducted at temperatures even below 700 K, high yields to syngas need substantially higher temperatures, typically 1100 K. The reaction products H_2, CO, and H_2O are for all practical purposes stable at reaction conditions.

5.5.2 Hydrogen Production from Hydrocarbons

Hydrogen production by catalytic steam reforming and partial oxidation of hydrocarbons has been the most efficient, economically and widely used process for the

production of hydrogen and hydrogen/carbon monoxide mixtures (synthesis gas or syngas). The process basically involves a catalytic conversion of the hydrocarbon and steam to hydrogen and carbon oxides. Since the process works only with light hydrocarbons, which can be vaporized completely without carbon formation, the feedstock used range from methane, to naphtha, to No. 2 fuel oil. The basic steps in conventional steam reforming are as follows:

1. Synthesis gas generation:
   A desulfurized hydrocarbon is mixed with process steam over a nickel-based catalyst in the reformer, where the endothermic reforming reaction occurs at 1175 K:

$$C_nH_m + nH_2O \rightarrow nCO + (n + m/2)H_2 \tag{5.9}$$

2. Supplemental hydrogen generation (water–gas shift):
   The synthesis gas enters the shift converter, where the exothermic water–gas shift reaction occurs at 475 to 675 K as follows:

$$CO + H_2O \rightarrow CO_2 + H_2 \tag{5.10}$$

3. Gas purification:
   CO_2 is removed in a scrubbing unit. Residual CO is converted in the methanator, where the following exothermic methanation reaction occurs:

$$CO + 3H_2 \rightarrow CH_4 + H_2O \tag{5.11}$$

The product hydrogen typically has a purity of 97–98%; 50% of the hydrogen is derived from H_2O when the hydrocarbon feedstock is methane and 64.5% when it is naphtha.

The typical composition of a synthesis gas at 0.7 MPa leaving a steam methane reformer is given in Table 5.3 (Caglar and Ozmen, 2000).

Hydrogen production by partial oxidation is similar to production by catalytic steam reforming. The process basically involves the conversion of steam, oxygen and hydrocarbons to hydrogen and carbon oxides. The process proceeds at moderately high pressures with or without a catalyst depending on the feedstock and process selected. The catalytic POX, which occurs at about 865 K, will work with feedstock ranging from methane to naphtha. The non-catalytic POX, which occurs

Table 5.3 Typical composition of synthesis gas at 0.7 MPa from a steam methane reformer

Component	Vol. (%)
H_2	34
CO	48
CO_2	17
N_2 and Ar	1
Total	100

at 1425–1590 K, can operate on hydrocarbons including methane, heavy oil, and coal. The synthesis gas step is slightly modified. A hydrocarbon feedstock is mixed with process steam and oxygen in the partial oxidation unit, and the following exothermic partial oxidation reactions occur:

$$C_nH_m + (n/2)O_2 \rightarrow nCO + (m/2)H_2 \quad (5.12)$$

$$C_nH_m + nH_2O \rightarrow nCO + (m/2)H_2 \quad (5.13)$$

$$CO + H_2O \rightarrow CO_2 + H_2$$

The product hydrogen typically has a purity of 93–98%.

There are three main steps:

1. Synthesis gas generation: Process in which light hydrocarbons are partially oxidized over a catalyst at about 875 K with oxygen and the carbon monoxide is shifted with steam to produce CO_2 and H_2.
2. Water–gas shift reaction: Processes in which heavy hydrocarbons such as heavy oil are partially oxidized without a catalyst present at about 1675 K, a temperature at which catalysts are not required to promote the reforming reaction.
3. Gas purification: Solid hydrocarbons such as coal are partially oxidized without a catalyst in the process.

The typical composition of the synthesis gas at 5.4 MPa leaving a POX reactor with heavy oil as feedstock is given in Table 5.4 (Caglar and Ozmen, 2000).

5.5.3 Hydrogen from Coal

Hydrogen production from carbonaceous feedstocks requires multiple catalytic reaction steps: For the production of high-purity hydrogen, the reforming of fuels is followed by two water–gas shift reaction steps, a final carbon monoxide purification and carbon dioxide removal. Steam reforming, partial oxidation and autothermal reforming of methane are well-developed processes for the production of hydro-

Table 5.4 Typical composition of synthesis gas at 5.4 MPa leaving POX reactor

Component	Vol. (%)
H_2	46
CO	46
CO_2	6
CH_4	1
N_2 and Ar	1
Total	100

gen. Stepwise steam reforming of methane for production of carbon monoxide-free hydrogen has been investigated at various process conditions by Choudhary and Goodman (2000). The process consists of two steps involving the decomposition of methane to carbon monoxide-free hydrogen and surface carbon in the first step followed by steam gasification of this surface carbon in the second step. The amount of carbon monoxide-free hydrogen formed in the first step hydrogen is produced in the second step of the reaction. The mixture of gases (primarily CH_4 and CO_2) can be separated or simply methanated and returned to the first step (Choudhary and Goodman, 1999).

Hydrogen derived from fossil fuels is not a clean, renewable resource. It may be easiest to sustain a transition to hydrogen by expanding commercially available, relatively inexpensive production processes, such as the manufacture of H_2 from coal. Coal is relatively abundant and could provide a low-cost feedstock for hydrogen. Coal represents a major energy source that can be transformed into transportation fuels and chemical feedstocks. A gasifier converts coal feedstock into gaseous components by applying heat and pressure to the coal in the presence of steam and oxygen.

A gasifier differs from a combustor in that the amount of oxygen inside the gasifier is carefully controlled such that only a relatively small portion of the fuel burns completely, minimizing the formation of carbon dioxide. The actual composition depends on the conditions in the gasifier and the type of feedstock. Typical coal syngas H_2 to CO ratios are in the 0.4:1 to 0.9:1 range. The gasification of coal is generally represented by the following reaction:

$$C + H_2O \rightarrow CO_2 + H_2 \tag{5.14}$$

The second step in the process consists of cleaning and shifting the CO to form hydrogen and CO_2 by reacting with steam. The overall reaction for converting the CO is the chemical shift reaction:

$$CO + H_2O \rightarrow CO_2 + H_2 \tag{5.15}$$

There are commercial or near commercial technologies for coal gasification processes used for hydrogen production. These are Koppers–Totzek and Texaco gasification processes.

In the Koppers–Totzek process, the polarized coal is rapidly partially oxidized with oxygen and steam at essentially atmospheric pressure under slogging con-

Table 5.5 Typical composition of synthesis gas from Koppers–Totzek gasifier

Component	Vol. (%)
H_2	29
CO	60
CO_2	10
N_2 and Ar	1
Total	100

Table 5.6 Typical composition of synthesis gas leaving the Texaco gasifier

Component	Vol. (%)
H_2	34
CO	48
CO_2	17
N_2 and Ar	1
Total	100

ditions. The typical composition of synthesis gas leaving the gasifier is given in Table 5.5 (Caglar and Ozmen, 2000).

The product hydrogen is about 2.8 MPa, with a purity higher than 97.5%. It is more efficient to gasify coal at elevated pressures.

The Texaco gasifier is a higher-pressure gasifier operating at around 5.5 MPa. By operating with a direct quench at this pressure, high steam content in the synthesis gas is desirable for use in the shift reaction for hydrogen production. The typical composition of synthesis gas leaving the Texaco gasifier is given in Table 5.6. The product hydrogen is about 4 MPa, with a purity higher than 97%.

5.5.4 Hydrogen from Water

Hydrogen can be obtained by direct electrolysis, by direct thermal conversion, thermochemically, photochemically, photoelectrochemically, and biochemically from water.

5.5.4.1 Direct Electrolysis of Water

Hydrogen production by electrolysis using electricity from fossil, nuclear, hydro, biomass, solar, and wind energy resources can be evaluated. But the hydrogen produced from electrolysis will in no way help reduce the pollution of the atmosphere if the electricity needed for the reaction is obtained through fossil fuels. Although presently not economically competitive with hydrogen produced from hydrocarbons, electrolytic hydrogen has several advantages such as high product purity and flexibility of operation. Non-polluting hydrogen would come from renewable sources like hydro, solar, wind and photocatalysis. Electrolysis produces extremely pure hydrogen, which is necessary for some types of fuel cells. But a significant amount of electricity is required to produce a usable amount of hydrogen from electrolysis.

Water electrolysis involves passing an electric current through water to separate it into hydrogen (H_2) and oxygen (O_2). Hydrogen gas rises from the cathode elec-

trode and oxygen gas collects at the anode electrode. The reactions involved in the electrolysis of water are:

Reduction cathode electrode:

$$4H_2O + 4e \rightarrow 2H_2 + 4OH^- \quad (5.16)$$

Oxidation anode electrode:

$$4OH^- \rightarrow 2H_2O + O_2 + 4e \quad (5.17)$$

Complete cell reaction:

$$H_2O + \text{Electricity} \rightarrow H_2 + 1/2\ O_2 \quad (5.18)$$

The values of the cathode and anode half-cell potentials are known to be 0.401 V and –0.828 V, respectively, at 298 K at a pH of 14. If the activities of water and the gaseous species are considered to be equal to unity, the cathode (E_c) and anode (E_a) potentials required according to Nernst equation will be:

$$E_c = -0.828 \quad - 0.059 \log a_{OH^-}$$
$$E_a = 0.401 \quad - 0.059 \log a_{OH^-}$$

The potential required to split water into H_2 and O_2, i.e., $(E_a - E_c)$ is equal to 1.229 V. Though the theoretical potential is 1.23 V for water electrolysis, in practice the actual water decomposition will occur only above 1.7 V. The extra potential, which is essential for the water decomposition, is called overpotential. Overvoltages are composed of activation or charge transfer overvoltage, concentration or diffusion or mass transfer overvoltage and resistance overvoltage. Overvoltage is evaluated mainly as a function of current and temperature (Viswanathan, 2006).

In general, an aqueous solution of caustic potash or soda is used as the electrolyte for water electrolysis. The nature of anode and cathode is decided based on their hydrogen and oxygen overvoltages in the electrolytic medium in addition to their stability in the particular medium. The cathode and anode are separated by a diaphragm, which prevents the mixing of hydrogen and oxygen gases produced at the cathode and anode surfaces respectively. The diaphragm should be stable in the electrolyte and minimizes the diffusion of gas molecules without affecting the conductivity of the medium. For ideal electrolyzers, heat is added to make up for the difference between the minimum electrical and total energy requirements. For practical electrolyzers enough heat is evolved due to cell inefficiencies to more than make up for the difference (Caglar and Ozmen, 2000; Viswanathan, 2006). When the temperature increases the reversible voltage decreases, whereas the thermoneutral voltage slightly increases with temperature. In general, the commercial industrial electrolytic cells operate between 333 and 353 K.

5.5.4.2 Direct Thermal Conversion of Water

Water can be decomposed thermally:

$$H_2O + \text{Heat} \rightarrow aH_2O + bH_2 \quad (5.19)$$

In Eq. 5.19, a and b are the mole fractions. At temperatures above 2500 K, the water molecules start dissociating into hydrogen and oxygen. This method (a) processes high thermal efficiency, (b) offers no or little environmental hazards, and (c) needs no immediate chemicals (Caglar and Ozmen, 2000). However, there are serious difficulties with direct thermal decomposition methods. Due to the increase of the kinetic energy of H_2O molecules with increasing temperature, this process requires more intensive energy.

5.5.4.3 Thermochemical Conversion of Water

The decomposition of water into hydrogen and oxygen can be achieved when energy is supplied in the form of heat and work. The positive value of ΔG^o decreases with increase in temperature, but rather slowly because of the nearly constant enthalpy change, as a function of temperature and ΔG^o becomes zero around 4700 K. This means that even the highest temperature available from a nuclear reactor, in the range of 1300 K, is not sufficient to decompose water. Therefore, single-step thermal decomposition of water is difficult unless other methods like electrolysis are then utilized. There is a two-step decomposition of water wherein a metal oxide, metal hydride or hydrogen halide is involved according to the equations:

$$H_2O + M \rightarrow MO + H_2 \quad (5.20)$$

$$MO \rightarrow M + 0.5O_2 \quad (5.21)$$

or

$$H_2O + M \rightarrow MH_2 + 0.5O_2 \quad (5.22)$$

$$MH_2 \rightarrow M + H_2 \quad (5.23)$$

However, even these two-step routes require temperatures on the order of 1273 K or more. Water cannot be decomposed in one or two thermochemical steps when the available temperature is below 1273 K.

High temperature (often exceeding 1000 K) drives the endothermic chemical reactions. Multistep cycles for water splitting are used because very high temperatures are required before an appreciable amount of water decomposes in single-step cycles. Thus, in one or more subsequent chemical reactions, the intermediary compounds can be recovered to the original substance, which is used repeatedly. The thermochemical water decomposition steps involve the following five principal reactions:

$$2H_2O + SO_2 + I_2 + 4NH_3 \rightarrow 2NH_4I + (NH_4)_2SO_4 \quad (5.24)$$

$$2NH_4I \rightarrow 2NH_3 + H_2 + I_2 \quad (5.25)$$

$$(NH_4)_2SO_4 + Na_2SO_4 \rightarrow Na_2S_2O_7 + H_2O + 2NH_3 \quad (5.26)$$

$$Na_2S_2O_7 \rightarrow SO_3 + Na_2SO_4 \quad (5.27)$$

$$SO_3 \rightarrow SO_2 + 0.5O_2 \quad (5.28)$$

These reactions take place at a range of temperatures: 325, 900, 675, 825, and 1140 K, respectively. In order to have this process viable 99.90 to 99.99% recovery must be achieved in each step to avoid the high cost of intermediary reagent replacement and to avoid the environmental problem of spoiling reagents, which cause pollution.

5.5.4.4 Photolytic Hydrogen Production

Photolytic hydrogen production processes use the energy in sunlight to separate water into hydrogen and oxygen. These processes are in the very early stages of research but offer long-term potential for sustainable hydrogen production with low environmental impact.

When water molecules adsorb energy at a rate of 68.3 kcal/mol of water from ultraviolet radiation, hydrogen in principle can be released. Photolysis, the splitting of water by light with the aid of photochemical electron transfer reagents analogous to chlorophyll has been described as "the most reagent solution" to the hydrogen production problem (Caglar and Ozmen, 2000).

5.5.4.5 Photochemical Hydrogen Production

A photochemical hydrogen production system is similar to a thermochemical system, in that it also employs a system of chemical reactants, which carry out the splitting of water. However, the driving force is not thermal energy but light, generally solar light. In this sense, this system is similar to the photosynthetic system present in green plants. One can effectively utilize photochemical means to promote endergonic (energy requiring) reactions. The sensitized oxidation of water by Ce^{4+} using irradiation of 254 nm light by the following reaction is known (Viswanathan, 2006):

$$Ce^{4+} + 0.5H_2O \rightarrow Ce^{3+} + 0.25O^2 + H^+ \qquad \Delta H = 3.8 \text{ kcal/mol} \qquad (5.29)$$

Ce^{3+} can be used with light of shorter wavelength to promote the hydrogen generation reaction:

$$Ce^{3+} + H_2O \rightarrow Ce^{4+} + 0.5H_2 + OH^- \qquad (5.30)$$

5.5.4.6 Photoelectrochemical Hydrogen Production

Photoelectrochemical (PEC) hydrogen production replaces one electrode of an electrolyzer with photovoltaic (PV) semiconductor material to generate the electricity needed for the water-splitting reaction. The efficiency loss of separate steps is done away with, as is the cost of the other components of a solar cell. PEC is elegantly simple, but finding PV materials both strong enough to drive the water split and stable in a liquid system presents great challenges for researchers. In its simplest

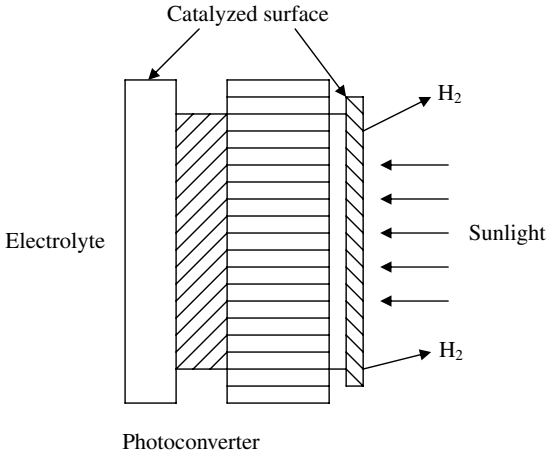

Fig. 5.3 Photoelectrochemical hydrogen production

form, a PEC hydrogen production cell consists of a semiconductor electrode and a metal counter electrode immersed in an aqueous electrolyte. When light is incident on the semiconductor electrode, it absorbs part of the light and generates electricity. This electricity is then used for the electrolysis of water.

In the illustration of a generic hydrogen photoelectrode shown in Fig. 5.3, sunlight shining on photoactive regions of the electrode produces an electric current to drive the hydrogen and oxygen evolution reactions (HER, OER) at opposite surfaces. Hydrogen photoelectrode operation represents a complex interaction of photovoltaic, optical, and electrochemical effects, and an important part of this research has been the development of integrated models combining these effects (Rocheleau and Vierthaler, 1994).

Iron oxide (Fe_2O_3) and tungsten oxide (WO_3) films have been studied and developed as candidate semiconductor materials for the PEC junction (photoanode). High-temperature synthesis methods, as reported for some high-performance metal oxides, have been found incompatible with multijunction device fabrication. A low-temperature reactive sputtering process has been developed instead. In the parameter space investigated so far, the optoelectronic properties of WO_3 films were superior to those of Fe_2O_3 films, which showed high recombination of photogenerated carriers (Miller et al., 2004).

5.5.5 Photocatalytic Hydrogen Production

Essentially, photocatalyzed reactions have generated considerable interest after the photocatalytic splitting of water on TiO_2 electrodes was first demonstrated by Fujishima and Honda in 1972. Subsequently, various kinds of photocatalysts have been employed for hydrogen production and remediation of pollutants from water.

Dispersed heterogeneous semiconductor surfaces provide a fixed environment that influences the chemical reactivity. Simultaneous oxidation and reduction reaction occurs on the surface of the catalyst during photoexcitation. The other advantages of this process are: the easy separation of catalyst after the reaction by centrifugation, availability of large surface area, low cost and stability. In heterogeneous photocatalytic systems, absorption of the light is an essential requirement for successful photocatalysis. In addition, it should be stable at the reaction conditions employed and it should be chemically inert. Among the available materials like metals, semiconductors and insulators, the semiconductors have been used because of their optimal band-gap, the band-edge positions are suitable for oxidation/reduction of water, and one can possibly use sunlight as an energy source to excite the electron from the valence band (Viswanathan, 2006).

Hydrogen has the potential to play an important role in future energy systems because of the possibility of producing hydrogen by splitting water using photocatalysts and solar energy. Photocatalytic water splitting with the use of solar energy is an attractive route for energy conversion because it converts water directly into hydrogen, the critical energy carrier of the future.

The method of catalytic photolysis of water, leading to obtainment of hydrogen, by using the oxide semiconductors, is an economic and clean technology; there are unlimited stores of material (water) and the needed energy (Sun). Therefore this method is very attractive. However, presently, renewable energy contributes only about 5% of the commercial hydrogen production primarily via water electrolysis, while the other 95% of hydrogen is mainly derived from fossil fuels (Ni et al., 2004). Photovoltaic water electrolysis may become more competitive as the cost continues to decrease with the technology advancement. Figure 5.4 shows the mechanism of dye-sensitized photocatalytic hydrogen production under visible light irradiation (Ni et al., 2007).

Some photocatalysts are used to adsorb visible light and then transmit the energy of appropriate wavelength and intensity to water molecules to liberate the constituent gases. The photolysis with a photo catalyst "X" can be expressed as follows:

$$H_2O + X + \text{Light} \rightarrow \text{Reduced X} + 2H^+ + 0.5O_2 \quad (5.31)$$

$$\text{Reduced X} + 2H^+ \rightarrow X + H_2 \quad (5.32)$$

$$\text{Overall reaction:} \quad H_2O + X + \text{Light} \rightarrow H_2 + 0.5O_2 + X \quad (5.33)$$

The photocatalysts "X" are some compound salts, compound semiconductors, photosynthetic dyes, some intact cells of some species of blue-green, green and red algae, or some photosynthetic bacteria (Caglar and Ozmen, 2000). Unfortunately, these systems typically are very inefficient, utilizing less than 1% of the incoming energy, and thus are very costly; although recent developments suggest that improvements are possible.

Production of hydrogen from an inexhaustible source, water, by a cheaper route has been under extensive investigation in recent years (Koca and Sahin, 2003). The requirement for the photoproduction of hydrogen using a semiconductor is the need for a hydrogen evolution catalyst on a semiconductor surface as reported by many

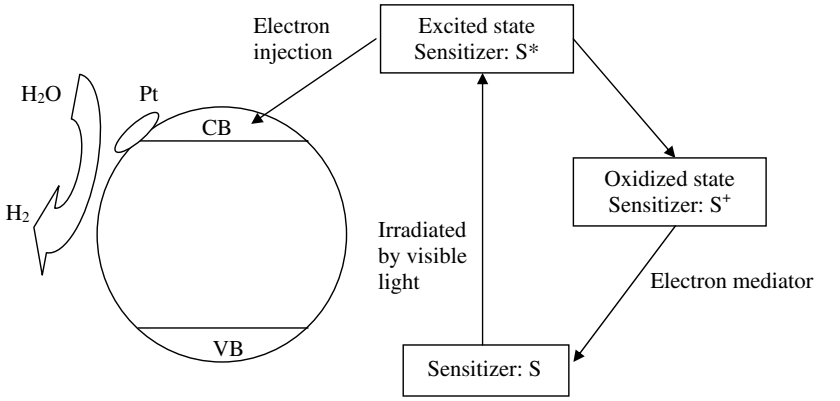

Fig. 5.4 Mechanism of dye-sensitized photocatalytic hydrogen production under visible light irradiation

research groups (Domen et al., 1982; Gurunathan, 2000). In view of the current importance of hydrogen as a clean chemical source, the discovery of new kinds of the photocatalysts for water decomposition is a very important issue (Sato et al., 2001). Selection of a suitable photocatalyst is an important criterion to establish the process as workable for the maximum quantity of hydrogen production. Extensive research has so far been performed, but stable photocatalysts found in the past two decades for the overall splitting of pure water to produce hydrogen and oxygen are confined to the transition metals involving Ti^{4+}, Zr^{4+}, Nb^{5+}, and Ta^{5+}; $SrTiO_3$ (Domen and Kudo, 1986), $A_2Ti_6O_{13}$ (A=Na, K, Rb) (Inoue et al., 1991; Ogura et al., 1997), $BaTi_4O_9$ (Kohno et al., 1998), $A_2La_2Ti_3O_{10}$ (A=K, Rb, Cs) (Takata et al., 1997a, 1997b), ZrO_2 (Sayama and Arakawa, 1993), $A_4Nb_6O_{17}$ (A=K, Rb) (Kudo et al., 1988), $Sr_2Nb_2O_7$ (Kudo et al., 2000), $ATaO_3$ (A=Na, K) (Kato and Kudo, 1999a; Ishihara et al., 1999), MTa_2O_6 (M=Ca, Sr, Ba) (Kato and Kudo, 1998, 1999b), and $Sr_2Ta_2O_7$ (Kudo et al., 2000) were active when combined with NiO or RuO_2 as a promoter (Sato et al., 2001). It will be greatly beneficial to demonstrate that metal oxides having other electronic structures are useful for photoassisted water decomposition. The development of visible light-active photocatalysts, therefore, has become one of the most important topics in photocatalysis research today (Jang et al., 2005).

Fujishima and Honda (1972) reported the photocurrent generation using semiconductor electrodes. Since then, scientific and engineering interests in semiconductor photocatalysis have grown significantly. In this system, electrons and holes are produced in a photocatalyst by incident light if the light energy is greater than the band-gap of the photocatalyst. Then, photogenerated electrons and holes react with water to produce H_2 and O_2, respectively, theoretically provided that the conduction band potential of the photocatalyst is more negative than the redox potential of H^+/H_2 (0 V vs. NHE; pH=0). The valence band potential is more positive that the redox potential of O_2/H_2O (1.23 V vs. NHE; pH=0) (Bak et al., 2002; Kudo, 2001;

Kida et al., 2004). Semiconductors have been utilized for this purpose in the form of electrodes (Desilvestro and Neumannspallart, 1985; Mackor and Blasse, 1981; Gringue et al., 1987; Ashokkumar et al., 1994), colloids (Kennedy and Dunnwald, 1983; Lee et al., 1984; Kamat and Fox, 1983; Kamat, 1989), powders (Ashokkumar and Maruthamuthu, 1989; Herrmann et al., 1986; Okamoto et al., 1985; Oosawa, 1984) and thin films (Fonash, 1981; Green, 1982; Faherburch and Bube, 1983).

The performance of semiconducting inorganic materials as a photocatalyst depends much on the physical properties of the particles such as crystallinity, size and morphology. The effect can be even more pronounced when using two or more materials together, since an intimate interaction between particles is more important in the multicomponent system (So et al., 2004).

Many chemical reactions have been tested using heterogeneous photocatalysts. These catalytic systems adsorb sunlight, transfer electrons and promote redox reactions (Cerveramarch, et al., 1992; Gurunathan, 2000; Moon et al., 2000; Tryk et al., 2000; Bamwenda and Arakawa, 2000; Namon et al., 1986; Gurunathan et al., 1997; Fletcher et al., 1984). Many photocatalyst systems have been tried for the production of hydrogen from water. Most of the photocatalyst systems studied recently include materials such as TiO_2 and B/TiO_2 (Moon et al., 2000), CeO_2–Ce^{+4}–Fe^{+3} (Bamwenda and Arakawa, 2000), CdS (Cerveramarch et al., 1992; De et al., 1996) or V_2O_4 (Namon et al., 1986). Gurunathan (2000) sensitized TiO_2 with CdS, Cu(II) ions, $Ru(bpy)_3^{+2}$, organic dyes and other photosensitizers and recorded 0.0225 ml/h g as the maximum hydrogen evolution rate. These are the ones that yielded maximum rates.

Table 5.7 Effect of the composition of CdS/ZnS photocatalyst system to the rate of hydrogen evaluation

CdS:ZnS	Wt.% CdS (mg)	Wt.% ZnS (mg)	Rate of H_2 (ml/h g)
1:0	100.0	00.0	2.80
4:1	80.0	20.0	4.20
3:1	75.0	25.0	8.30
2:1	66.6	33.4	15.60
3:2	60.0	40.0	12.50
1:1	50.0	50.0	5.40
2:3	40.0	60.0	4.50
1:2	33.4	66.6	3.80
1:3	25.0	75.0	3.30
1:4	20.0	80.0	1.50
0:1	00.0	100.0	0.00

5.5.5.1 Photocatalytic H_2 by Direct Sunlight from Sulfide/Sulfite Solution

The photocatalytic hydrogen production from a sulfide/sulfite solution is one of the photocatalytic processes of interest recently for hydrogen production. A different situation would be where waste materials have to be eliminated or used to produce energy and useful products. Sulfide and sulfite, undesirable waste products in fossil fuel technology, should be explored as a source of hydrogen. In that case, most of the raw materials could be considered as zero or negative. For instance, a large amount of sulfide and sulfite produced in oil refineries is inconvenient, but can be used as a sacrificial material to produce hydrogen by photocatalytic reactions (Fletcher et al., 1984).

Koca and Sahin (2002) carried out different series of experiments in order to compare the amounts of hydrogen evolved by different compositions of CdS/ZnS. Table 5.7 shows the rates of hydrogen evolution, which was dependent upon the percentage of CdS and ZnS in each photocatalyst. These results show that 33% ZnS is the most active (Koca and Sahin, 2002). CdS was sensitized with a co-precipitation by using a hot mixture of $Cd(CH_3COOH)_2$, $Zn(CH_3COOH)_2$ and Na_2S; Zn^{+2} ions loaded on CdS, and this enhanced hydrogen production efficiency of the photocatalyst system.

5.5.5.2 Photocatalytic H_2 from Water over Titania Aerogels Under UV Irradiation

Aerogels are light solid materials. Their unique properties include extremely low densities combined with large porosities and surface areas. One potential application of aerogels is in photocatalytic processes like photodecomposition of organic pollutants in water or air. For such application a semiconducting material is needed as a solid matrix of aerogel. Data from literature point to titania and hybrid titania-silica aerogels as attractive photocatalysts or carriers for further doping with metals. Titania aerogels were used in photodegradation of such compounds like p-chlorophenol, 4-hydroxybenzoic acid (Malinowska et al., 2003a) and p-nitrophenol (Malinowska et al., 2003b). Dagan and Tomkiewicz (1994) proved that titania aerogels can be much more active in the photodegradation process of the simple aromatic compound, salicylic acid, in comparison with commercial P25 Degussa TiO_2.

Piotrowska and Walendziewski (2005) carried out experiments with these aerogels in the process of photocatalytic hydrogen production. The highest activity they have obtained was using titania aerogels, with platinum in the aqueous solution of methanol (10 ml CH_3OH/400 ml H_2O). After 55 min of the tests exposure they obtained 6.59 mmol of H_2 over titania aerogel. Titania aerogels impregnated with platinum show a similar efficiency in the process of photocatalytic hydrogen production by water splitting as commercial TiO_2 P25 impregnated with Pt. The obtained results indicated that titania aerogels are a promising catalytic material in photocatalytic production. The type of solvent used in aerogels preparation has

no influence on catalytic activity. Platinum deposited over titania aerogel gives a higher activity water-splitting photocatalyst in comparison to palladium and nickel deposited over titania aerogel (Piotrowska and Walendziewski, 2005).

5.5.5.3 Photocatalytic H_2 from Suspension of Spinel Powders AMn_2O_4

Visible light-induced hydrogen evolution over the spinel oxide AMn_2O_4 (A=Cu, Zn) has been investigated in the presence of sulfide and/or sulfite as hole scavengers (Bessekhouad and Trari, 2002). The platinized catalysts showed a better performance, with an increase of 30% of H_2 production obtained. Over time, the oxidation of sulfide does not maintain a constant hydrogen evolution because of the formation of the yellow polysulfide S_n^{2-} ions that form an optical filter reducing the light absorption of AMn_2O_4 and competing with the reduction of H_2O molecules. SO_3^{-2} acts as a regenerative agent and keeps the solution transparent. At lower temperatures, SO_3^{-2} worked as a hole scavenger and exhibited a higher gas production. Higher specific surface area of $ZnMn_2O_4$ powder, obtained by co-precipitation, does not improve the H_2 production and suggests that both the depletion layer thickness and the carrier diffusion length are smaller than the average crystallite size.

5.5.5.4 Zirconium-Titanium Phosphates for H_2 by Photo-Induced Water Splitting

Due to the UV light absorption property of titanium phosphate containing mesoporous materials with large surface areas and ion exchange capacity, they are candidates for use as photocatalysts, especially for hydrogen generation by water decomposition (Bhaumik and Inagaki, 2001). In the case of mesoporous zirconium-titanium phosphates (ZTP), the homogeneous pore distribution including the large internal surface area makes such materials accessible to the water molecule, and a highly charged structure existing on the surface facilitates the charge separation process essential for the decomposition of water. Inagaki and co-workers examined the photocatalytic splitting of water for hydrogen production using Pt-loaded ZTP mesoporous materials under UV-vis light irradiation. The results of photocatalytic decomposition of water for hydrogen generation evidently suggest that mesoporous ZTP materials are possible candidates for photocatalysts for hydrogen production (Kapoor et al., 2005).

5.5.5.5 Light-Induced Production of H_2 from Water by Catalysis

A ruthenium-containing melanoidin (a condensation product of amino acids and carbohydrates) was found to photocatalyze hydrogen production from water under light irradiation with $\lambda < 320$ nm, in the presence of EDTA as an electron donor and methyl viologen as an electron relay. The Ru-melanoidin photocatalyst is stable under prolonged irradiation times and, due to its insolubility in water, is suitable for

recycling. Ru-containing melanoidin can act as a cheap, stable and reasonably efficient photosensitizer for photocatalytic hydrogen production from water. It is also conceivable that a support mounted catalyst system would allow hydrogen production in a flow system (Serban and Nissenbaum, 2000).

Cadmium sulfide is one of the most well-studied semiconductors for solar energy utilization. It possesses a relatively narrow band-gap of approximately 2.4 eV; its conduction band-edge is more negative than the H_2/H_2O redox potential, thus it is able to evolve H_2 from water when irradiated with visible light (Buhler et al., 1984). However, the activity of CdS is generally poor in the absence of electron donors such as Na_2S and H_3PO_2, because photogenerated holes in the valence band tend to react with CdS itself (photocorrosion). In an attempt to improve its activity, $LaMnO_3$/CdS nanocomposite was developed as a new type of visible light-sensitive photocatalyst that can produce hydrogen from water containing electron donors. The nanocomposite catalyst, prepared by a reverse micelle method, was found to show high photocatalytic activity, as compared to that of CdS; on the other hand, $LaMnO_3$ showed no photocatalytic activity. The proposed energy diagrams for the $LaMnO_3$/CdS composite, based on the results obtained from photoemission yield measurements, suggest that photogenerated holes in the valence band of CdS could move to that of $LaMnO_3$, thus separating photogenerated charge carriers and improving the activity (Kida et al., 2003).

5.5.5.6 Production of Hydrogen from Photocatalytic Water Splitting by Using TiO_2

Photocatalytic water splitting using TiO_2 for hydrogen production offers a promising way for clean, low-cost and environmentally friendly production of hydrogen by solar energy. TiO_2 has been widely used in photocatalysis, because of its favorable band-gap energy (3.2 eV in anatase) and its high stability in aqueous solution under UV irradiation (Galinska and Walendziewski, 2005).

It is well-known that nano-TiO_2 is one of the suitable semiconductors for photocatalyst and has been applied in various photocatalytic reactions (Fujishima et al., 2000). However, its properties, not only the photoefficiency or activity but also the photoresponse, are not sufficient (Kawai and Sakata, 1980). Meanwhile, the high recombination ratio of photoinduced electron–hole pairs also reduces its catalytic efficiency. Therefore various modifications have been performed on nano-TiO_2 to promote its catalytic ability and develop new photocatalytic functions (Ohno et al., 1996; Litter, 1999; Navvio et al., 1999; Choi et al., 1994; Nishikawa et al., 2001; Amiridis et al., 1999).

Since the discovery of photoelectrochemical splitting of water on titanium dioxide (TiO_2) electrodes (Fujishima and Honda, 1972), semiconductor-based photocatalysis has received much attention. Although TiO_2 is superior to other semiconductors for many practical uses, two types of defects limit its photocatalytic activity. Firstly, TiO_2 has a high band-gap ($E_g = 3.2$ eV), and it can be excited only by UV light ($\lambda < 387$ nm), which is about 4–5% of the overall solar spectrum. Thus, this restricts the use of sunlight or visible light (Kormann et al., 1988). Secondly, the

high rate of electron-hole recombination at TiO_2 particles results in a low efficiency of photocatalysis (Linsebigler et al., 1995). To overcome these limitations of TiO_2, many attempts have been made, for example, depositing of noble metals, mixing metal oxides with TiO_2 and doping selective metal ions into the TiO_2 lattice (Anderson and Bard, 1995; Borgarello et al., 1982; Ranjit et al., 1999; Moon et al., 2001). The advantage of doping the metal ions into TiO_2 is the temporary trapping of the photogenerated charge carriers by the dopant and the inhibition of their recombination during migration from inside the material to the surface. The effect of metal ion doping strongly depends on many factors such as the dopant concentration, the distribution of the dopants, the configuration of doping ions and so on (Borgarello et al., 1982). There have been many studies on transition metal, rare-earth and noble metal ion dopants in TiO_2, but reports on alkaline-earth metal ion-doped TiO_2 and their photocatalytic properties have seldom been seen (Talavera et al., 1997).

Kiwi and Morrison (1984) investigated the effect of lithium doping on TiO_2, towards water photocleavage experiments. It showed that Li doping promoted conduction band electron-transfer. This effect was likely to contribute to the observed enhancement in hydrogen generation and oxygen photoadsorption with increased Li content. Displacement of the conduction band of TiO_2 samples to more positive values took place upon Li doping (Kiwi and Morrison, 1984).

Abe et al. (1999) illuminated an aqueous suspension of TiO_2/Pt with an Hg arc lamp and observed H_2 production in the absence of O_2 production. An unspecified elemental analysis excluded carbonaceous contaminants, and the source of the electron donor was concluded to be Ti^{4+} cations (Abe et al., 1999).

Sodium carbonate (Na_2CO_3) addition to a Pt/TiO_2 suspension significantly promotes stoichiometric photodecomposition of liquid water (Sayama and Arakawa, 1992a). This procedure was also applicable to many other photocatalyst systems such as M/TiO_2, M/Ta_2O_5, M/ZrO_2, M/$SrTiO_3$, etc. (M = metal or metal oxide) (Sayama and Arakawa, 1992b; Sayama and Arakawa, 1996). Water was decomposed efficiently and stoichiometrically to H_2 and O_2 using a 3 wt.% NiO_x/TiO_2 photocatalyst under real solar light irradiation by this Na_2CO_3 addition method (Arakawa and Sayama, 2000). The main role of Na_2CO_3 for water splitting is the significant acceleration of O_2 desorption from the oxide semiconductor surface via peroxycarbonate intermediates which are formed by the reaction of surface carbonate species and positive holes in the valence band area of the oxide semiconductor catalyst by photoexcited charge separation under irradiation.

Wider band-gap materials such as TiO_2, ZnO, $SrTiO_3$ and ZnS showed good photostability but lower efficiency due to limited light harvesting when using the solar light (Reber and Meier, 1984). Small and medium band-gap materials such as CdS, CdSe, MoS_2 and Cu_2O experienced severe photoanodic corrosion. Thus, one of methods to overcome these drawbacks was to mix two or more semiconducting materials with different band-gaps and band positions so that an effective charge separation could occur between the contacting particles (Serpone et al., 1984). The intercalation of nanosized Fe_2O_3, TiO_2, and CdS particles into the interlayer of layered compounds such as $HNbWO_6$ or $HTaWO_6$ has been reported (Wu et al., 1999a,

Table 5.8 Photocatalytic hydrogen production from water over Cr- and Fe-doped $La_2Ti_2O_7$ under visible light irradiation ($\lambda > 420$ nm)

Photocatalysts	H_2 production rate[a] (μmol/h)
$Pt/La_2Ti_2O_7$	0
$Pt/Cr\text{-}La_2Ti_2O_7$ (Cr/La = 0.01)	15
Pt/Cr, $Sb\text{-}La_2Ti_2O_7$ (Cr/La = 0.01)	4
$Pt/Cr\text{-}La_2Ti_2O_7$ (Cr/La = 0.05)	8
$Pt/Fe\text{-}La_2Ti_2O_7$ (Fe/La = 0.01)	10
$Pt/Fe\text{-}La_2Ti_2O_7$ (Fe/La = 0.05)	5

[a]Measured in outer irradiation cell from a 500 W high-pressure Hg lamp; H_2O 100 ml + MeOH 50 ml, catalyst 0.5 g, 420 nm cutoff filter was used; 1 wt.% of Pt was loaded using H_2PtCl_6 by photoplatinization

1999b, 2001). The photoactivity improved markedly over those of unintercalated photocatalyst particles, which was ascribed to an effective separation of photogenerated electrons and holes due to their rapid diffusion (Jang et al., 2005). The intercalated nanoparticles were the production of hydrogen from water containing a sacrificial agent (CH_3OH) under visible light irradiation with quantum yields as high as 10% (Wu et al., 2001).

Wu et al. (1999b) reported that the intercalated Fe_2O_3 showed photocatalytic activity of H_2 evolution from a CH_3OH–H_2O solution by transfer of the photoelectron from Fe_2O_3 to the host layered compound, which decreased the recombination of electrons and holes under visible light irradiation. However, it was found in this work that hydrogen evolution under visible light was not due to photocatalytic decomposition of water (Wu et al., 1999b).

Photocatalytic water splitting is observed at the presence of applying EDTA and Na_2S as the sacrificial reagents. They act as effective hole scavengers; however, they are oxidized due to OH radicals, preventing oxygen formation and the recombination of the reaction of oxygen with hydrogen (Galinska and Walendziewski, 2005).

A few oxides are also active under visible light such as $HPb_2Nb_3O_{10}$ (Yoshimura et al., 1993), $MgWO_x$ (Hwang et al., 2002), and $Ni_xIn_{1-x}TaO_4$ (Zou et al., 2001), yet their activities are very low. Recently, some UV-active oxides turned into visible light photocatalysts by substitutional doping of C, N, and S, i.e., $TiO_{2-x}N_x$ (Asahi et al., 2001), $TiO_{2-x}C_x$ (Khan et al., 2002), TaON (Hitoki et al., 2002) and $Sm_2Ti_2O_5S_2$ (Ishikawa et al., 2002). Lee and co- workers studied cation-hybrid photocatalysts based on $La_2Ti_2O_7$ (Lee et al., 1984). Among various types of dopants, only Cr and Fe showed intense absorption in the visible light region ($\lambda > 420$ nm), over which H_2 was produced photocatalytically in the presence of methanol. Table 5.8 shows photocatalytic hydrogen production values from water over Cr- and Fe-doped $La_2Ti_2O_7$ under visible light irradiation ($\lambda > 420$ nm) (Hwang et al., 2004).

5.5.5.7 H_2 from Photocatalytic Water Splitting Using Photobiocatalytic Method

Hydrogen can be generated from water photocatalytically, photobiologically, and photoelectrochemically. The photobiocatalytic method is a novel method of hydrogen production by coupling an inorganic semiconductor with a bacterial enzyme (Gurunathan, 2000). Some researchers have reported on photocatalytic hydrogen production with Cu(II)/WO_3 (Maruthamuthu and Ashokkumar, 1988; Maruthamuthu et al., 1989), Cu(II)/Bi_2O_3 (Maruthamuthu et al., 1993), Rh[III]/Fe_2O_3 (Gurunathan and Maruthamuthu, 1995), Pt/SnO_2 (Gurunathan et al., 1997) using methyl viologen and reported photobiocatalytic hydrogen production using undoped Bi_2O_3 coupled with photosynthetic bacteria (Maruthamuthu et al., 1992). It is discussed that the nitrogenase enzyme of the bacterial cells is responsible for catalyzing hydrogen production. Sensitization of TiO_2 was performed in three ways:

1. Using organic dyes
2. Using Cu(II) ion doping
3. Loading with low band-gap semiconductors (CdS)

In the four components, i.e., TiO_2/MV^{2+}/electron donor/bacterial cells, each of the last three components has its own specific function and each facilitates the other's role, thereby enhancing the yield of hydrogen production. It was found that with sensitized TiO_2, there is a higher amount of hydrogen production than with the naked TiO_2. Among the sensitizers used, Rhodamine B and $Ru(bpy)_3^{2+}$ exhibited higher efficiencies compared with other sensitizers, as well as other methods of sensitization (2 and 3) (Gurunathan, 2000).

Nikandrov et al. (1988) coupled bacterial enzyme from *Thiocapsa roseopersina* to TiO_2 and observed an efficient photobiocatalytic hydrogen production. Thus a better catalyst has an origin in biology, i.e., bacterial enzyme which catalyzes the hydrogen evolution.

TiO_2 was coupled to intact bacterial cells of *Rhodopseudomonas capsulata* species as photocatalyst for hydrogen production using light of $\lambda > 400$ nm. The semiconductor-bacterial cells system is then subjected to hydrogen in aqueous solution under visible light using MV^{2+} (methyl viologen dichloride hydrate) as an electron relay with or without an electron donor (Gurunathan, 2000).

5.5.5.8 Photocatalytic H_2 from Sewage Sludge

Among various types of biomass, sewage sludge is more difficult to utilize due to its lesser quality. Nevertheless, some attempts have been made for converting sewage sludge into fuel, e.g., by thermochemical pyrolysis (Urban and Antal, 1982; Stolarek and Ledakowicz, 2001; Midilli et al., 2002) or solubilization methods (Yokoyama et al., 1987; Suzuki et al., 1988; Suzuki et al., 1990; He et al., 2000). Kida et al. (2004) investigated photocatalytic hydrogen production from a digested

sewage sludge solubilized in hot-compressed water (573 K) in order to develop a low-cost sacrificial agent for CdS-based photocatalysts from biomass. H_2 evolution occurred over a $LaMnO_3$/CdS composite photocatalyst under Xe lamp irradiation from water containing the solubilized sewage sludge. The amount of evolved H_2 reached more than 30 mmol/g catalyst for a 200 h reaction; on the other hand, no H_2 was formed in the absence of the solubilized sewage sludge. The H_2 evolution rate was comparable to that when typical Na_2S–Na_2SO_3 sacrificial agents were used, suggesting the applicability of a biomass-derived sacrificial agent for photocatalysis. Organic compounds, such as methanol and formic acid, contained in the solubilized sewage sludge are responsible for the H_2 evolution observed (Kida et al., 2004).

5.5.6 Solar-Powered Hydrogen Generation

Solar radiation is the largest renewable source on earth. A comparative overview of the selected integrated systems indicated that the Sun is the primary source of energy for many of the hydrogen demonstration projects. Electrochemical water splitting powered by photovoltaic arrays produces molecular hydrogen at the cathode, while organic compound oxidation under mild conditions takes place at the anode in competition with the production of oxygen. Hydrogen can be obtained from water by directly connecting a photovoltaic module to a hydrogen generator, with a solid polymer electrolyte (SPE).

The electrolysis of water using cells with a SPE is a very efficient method of producing hydrogen. SPE water electrolysis is one of the ways for producing hydrogen with comparatively high levels of efficiency and with compact equipment. SPE is composed of a membrane, cathode and anode which produce hydrogen by providing pure water to one side of a polymer ion exchange film, which is put between the anode and cathode.

If hydrogen is produced via solar photovoltaic (PV)-powered water electrolysis, it would be possible, in principle, to provide energy on a global scale, with essentially no greenhouse gas emission and very low local pollution.

Accordingly, the operation of electrolyzers with intermittent sources of solar energy and the various possibilities for matching photovoltaic current with the characteristics of the electrolyzer was one of the recurrent design issues in such projects. Most of the electrolyzers were of the alkaline type and operated at low pressure.

Concentrated solar radiation can be used for gasification of biomass to produce hydrogen. A detailed review with many references of the technology describes solar gasification of carbonaceous materials to produce a syngas quality intermediate for production of hydrogen and other fuels (Midilli et al., 2000). Shahbazov and Usupov (1994) have shown a good yield of hydrogen from agricultural wastes using a parabolic mirror reflector.

5.5.7 Hydrogen from Hydrogen Sulfide

Sulfur is recovered from H_2S by partial oxidation by the Claus process, and low-quality steam is produced utilizing the heat of reaction. Efforts to produce both hydrogen and sulfur from hydrogen sulfide have been made in recent years through a diverse variety of technologies. These involve thermal, thermochemical, electrochemical, photochemical and plasmochemical methods (Zaman and Chakma, 1995). H_2S potentially has economic value if both sulfur and hydrogen can be recovered. Various techniques that are at different stages of development can be considered for the decomposition of H_2S and they can be basically grouped into categories of thermal, thermochemical, electrochemical, photochemical and plasmochemical methods (Baykara et al., 2005, 2007).

Thermolysis of H_2S was carried out in an open tubular reactor quartz tube with argon/H_2S feed over a wide composition spectrum (20–100% H_2S) at four temperatures (1030–1070 K). These experiments show that the reaction is essentially first order in H_2S partial pressure. Hydrogen yield also increases monotonically with feed composition at all temperatures (Adesina et al., 1995).

Petrov (1991) suggested the idea for using H_2S for production of hydrogen and sulfur in the electrolytic stage of the solar-wind-hydrogen energy systems (SWHES).

A thermodynamic model for the partial oxidation of H_2S was used to study product compositions attainable in the superadiabatic partial oxidation regime. Superadiabatic partial oxidation techniques permit attainment of operating temperatures significantly in excess of the adiabatic temperature of the incoming reactants (Slimane et al., 2004a).

Superadiabatic partial oxidation (combustion) process is the thermal decomposition of H_2S in H_2S-rich waste streams to high-purity hydrogen and elemental sulfur (Slimane et al., 2002). In the superadiabatic combustion (SAC) process, some part of the H_2S is combusted to provide the thermal energy required for the decomposition reaction, as indicated by the following two reactions:

$$2H_2S + O_2 \rightarrow 2S + H_2O \qquad \Delta H = -189\,269 \text{ kJ/mol} \tag{5.34}$$

$$H_2S \rightarrow H_2 + S \qquad \Delta H = +17\,423 \text{ kJ/mol} \tag{5.35}$$

As can be seen from Eqs. 5.34 and 5.35, each molecule of H_2S reacting with oxygen can provide enough energy to dissociate up to 10 additional molecules of H_2S in an available reactor under suitable conditions.

The SAC, also known as filtration combustion, consists of combustion of a fuel gas-oxidant mixture in a porous ceramic medium with a high thermal capacity (Kennedy et al., 1995). The intense heat exchange between burning gas mixture and the porous medium permits the accumulation of combustion energy in the solid matrix. Figure 5.5 shows hydrogen recovering from H_2S via the superadiabatic combustion (SAC) process.

5.5.7.1 Sulfur–Iodine Thermochemical Water-Splitting Process

The sulfur–iodine thermochemical water-splitting cycle (S–I cycle) developed for hydrogen production from water is fundamentally based on the following three chemical reactions (Wang, 2007):

$$H_2SO_4 \rightarrow H_2O + SO_2 + 0.5O_2 \quad (5.36)$$

$$2H_2O + SO_2 + I_2 \rightarrow H_2SO_4 + 2HI \quad (5.37)$$

$$2HI \rightarrow H_2 + I_2 \quad (5.38)$$

This process proposes to replace the H_2SO_4 decomposition with a reaction between H_2S and H_2SO_4 and the replacement gives rise to a H_2S-splitting cycle that produces H_2 and elemental S from H_2S, shown as follows:

$$H_2S + H_2SO_4 \rightarrow S + SO_2 + 2H_2O \quad (5.39)$$

$$2H_2O + I_2 + SO_2 \rightarrow H_2SO_4 + 2HI \quad (5.40)$$

$$2HI \rightarrow H_2 + I_2 \quad (5.41)$$

Combined with the reactions such as:

$$O_2 + S \rightarrow SO_2 \quad (5.42)$$

$$SO_2 + 0.5O_2 \rightarrow SO_3 \quad (5.43)$$

$$SO_3 + H_2O \rightarrow H_2SO_4 \quad (5.44)$$

This new cycle cannot only produce more H_2 and extra H_2SO_4 but also facilitate a flexible H_2 to H_2SO_4 production ratio. In gas plants, H_2 from H_2S splitting is an alternative clean fuel. Environmentally, H_2 production based on this H_2S-splitting cycle is carbon-free.

The sulfur–iodine (S–I) thermochemical water-splitting cycle is one of the most studied cycles for hydrogen (H_2) production (Huang and Raissi, 2005). The S–I cycle consists of four sections: (I) acid production and separation and oxygen purification, (II) sulfuric acid concentration and decomposition, (III) hydroiodic acid (HI) concentration, and (IV) HI decomposition and H_2 purification. Section II of the cycle is an endothermic reaction driven by the heat input from a high-temperature source. Analysis of the S–I cycle in the past thirty years has focused mostly on the utilization of nuclear power as the high-temperature heat source for the sulfuric acid decomposition step. Thermodynamic as well as kinetic considerations indicate that both the extent and rate of sulfuric acid decomposition can be improved at very high temperatures (in excess of 1275 K) available only from solar concentrators. These new sulfuric acid decomposition processes are simpler and more stable than previous processes and yield higher conversion efficiencies for the sulfuric acid decomposition and sulfur dioxide and oxygen formation. Figure 5.5 shows the sulfur–iodine cycle for hydrogen production (Huang and Raissi, 2005; Balat and Ozdemir, 2005).

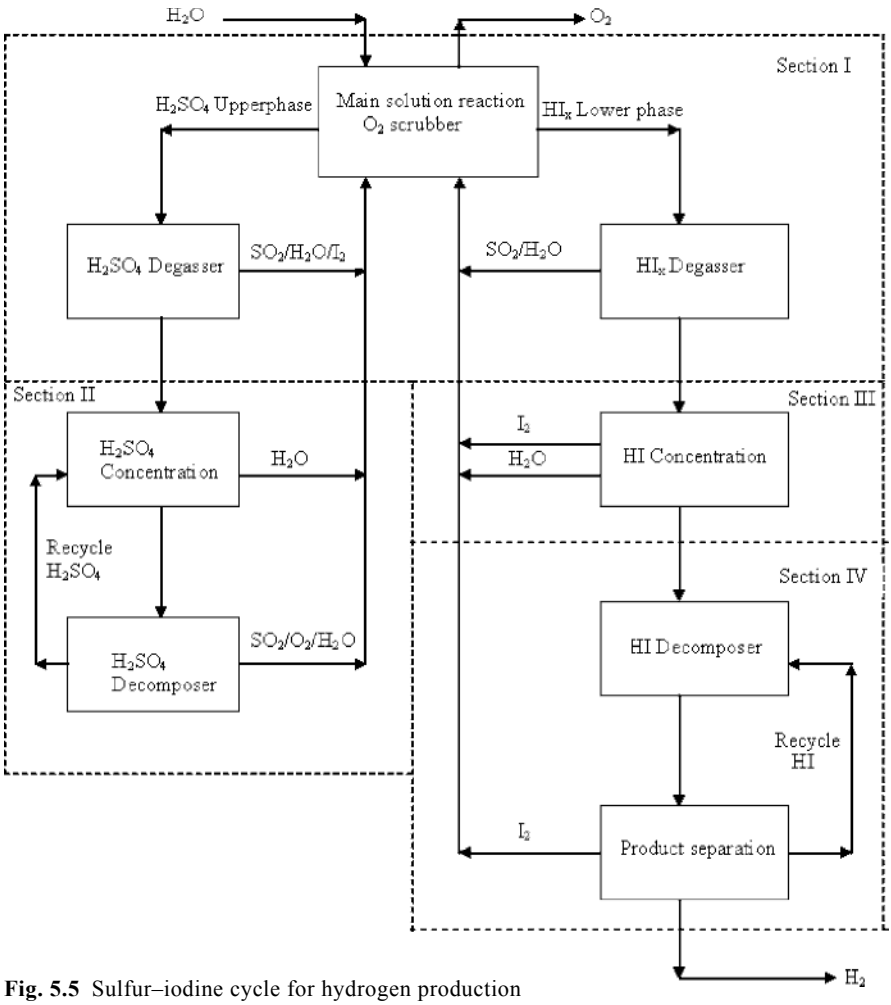

Fig. 5.5 Sulfur–iodine cycle for hydrogen production

5.5.7.2 Pyrolysis of Hydrogen Sulfide

Catalytic or non-catalytic, thermal decomposition appears to be the most direct process for obtaining both hydrogen and sulfur from H_2S. The reactions involved are highly endothermic and the equilibrium conversion corresponding to a temperature range of 1100–1400 K would be between 10–30%. The conversion level can be increased by catalysis and by removal of H_2 and S during reaction. Membrane, thermal diffusion and solar technologies need more development since they seem to be quite promising (Baykara et al., 2005).

Production of hydrogen by direct decomposition of hydrogen sulfide has been studied extensively (Clark et al., 1995; Zaman and Chakma, 1995; Luinstra, 1996). Hydrogen sulfide decomposition is a highly endothermic process and equilibrium

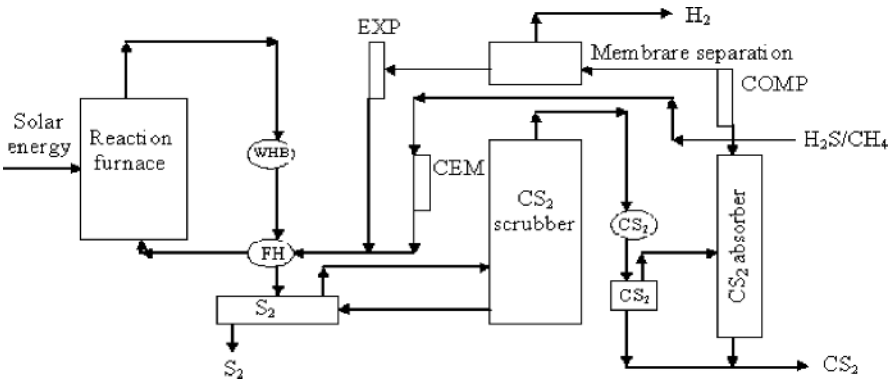

Fig. 5.6 CH_4/H_2S reforming for hydrogen production

yields are poor (Clark et al., 1995). At temperatures less than 1775 K, the thermodynamic equilibrium is unfavorable toward hydrogen formation. However, in the presence of catalysts such as platinum–cobalt (at 1275 K), disulfides of Mo or W at 1075 K (Kotera et al., 1976), or other transition metal sulfides supported on alumina (at 775–1075 K), H_2S decomposition proceeds rapidly (Kiuchi et al., 1982; Bishara et al., 1987; Al-Shamma and Naman, 1989; Megalofonos and Papayannakos, 1997).

5.5.7.3 Hydrogen Sulfide Reformation of Natural Gas

Hydrogen gas can be obtained by direct thermolysis of methane and pyrolysis of hydrogen sulfide. Direct thermal dissociation of methane and H_2S does not generate greenhouse gases. However, compared to the steam methane reforming (SMR) process, thermolysis of CH_4 and H_2S generates smaller amounts of hydrogen per mole of methane and hydrogen sulfide reacted. The reaction of H_2S with methane can be thought of as the sulfur analog of the SMR process, as indicated by the following two reactions (Hacisalihoglu et al., 2008):

$$H_2S \rightarrow H_2 + 0.5S_2 \qquad \Delta H = +79.9 \text{ kJ/mol} \qquad (5.45)$$

$$CH_4 + 2S_2 \rightarrow CS_2 + 2H_2S \qquad \Delta H = -107 \text{ kJ/mol} \qquad (5.46)$$

The overall reaction may be written as follows:

$$CH_4 + 2H_2S \rightarrow CS_2 + 4H_2 \qquad \Delta H = +232.4 \text{ kJ/mol} \qquad (5.47)$$

The byproduct obtained from the overall reaction is carbon disulfide (CS_2). The reaction between CH_4 and H_2S given with Eq. 5.47 is the well-known methane process for production of CS_2. Most commercial CH_4–sulfur processes employ silica gel/aluminum catalyst for CS_2 production. The reaction of CH_4 with sulfur is thermodynamically favorable for CS_2 formation, and conversion is usually in the range of 90 to 95% with respect to methane (Arpe, 1989). The industrial CH_4–sulfur pro-

Table 5.9 Main hydrogen storage methods and techniques

Storage method	Storage condition
Liquid hydrogen in cryogenic tanks	At 21 K
High-pressure gas cylinders	Up to 800 bar
Adsorbed hydrogen on materials	At $T < 100$ K
Absorbed on interstitial sites in a host metal	At ambient pressure and temperature
Oxidation of reactive metals, e.g., Li, Na, with water	At ambient pressure and temperature
Chemically bonded in covalent and ionic compounds	At ambient pressure
Chemically bonded to either metal or liquid hydrides	At ambient pressure
Chemically carbon bonding	At ambient pressure

cess operates in the temperature range of 775 to 925 K and pressure range of 4 to 7 atm. Figure 5.6 shows the H_2S/CH_4 reforming process for hydrogen production (Huang and Raissi, 2005; Balat and Ozdemir, 2005).

5.6 Storage of Hydrogen

Hydrogen has the highest energy density per unit of weight of any known fuel (excluding nuclear reactions), but 1 g of hydrogen gas occupies about 111 of space at atmospheric pressure, so its storage for vehicular use presents problems. There are a few different approaches for hydrogen transportation and storage. Hydrogen can be stored as a compressed gas (up to 800 bar), as a liquid (at 21 K) and in solid-state compounds. The first two methods are established technologies with several limitations, the most important of which is their energy-intensive character. Conventional storage systems consist of classical high-pressure tanks and insulated liquid hydrogen systems. Compressing hydrogen is similar to compressing natural gas, though as hydrogen is less dense the compressors need very high-quality seals. The main disadvantages of using hydrogen as a fuel for automobiles are huge on-board storage tanks, which are required because of hydrogen's extremely low density. Hydrogen may be stored on board a vehicle as compressed gas in ultrahigh-pressure vessels, as a liquid in cryogenic containers, or as a gas bound with certain metals in metal hydrides. Liquefaction by the Linde cycle, for example, consumes nearly 30% of the total energy contained in the hydrogen and in addition requires expensive equipment and energy to retain hydrogen in the liquid state. Up to 40% of the energy content in the hydrogen can be lost during the liquefaction operation. The liquid hydrogen storage is very expensive in comparison to other methods. The advantage of liquid hydrogen is its high energy-to-mass ratio, three times that of gasoline. However, it is difficult to store and the insulated tank required may be large and bulky (Demirbas, 2007).

Table 5.10 Characteristics of six basic hydrogen storage methods

Storage media	Pressure (bar)	Temperature (K)	Maximum capacity wt.%
Composite cylinder	800	298	13
Liquid hydrogen	1	21	100
Metal hydrides	1	298	2
Complex hydrides	1	298	18
Alkali with water	1	298	14
Physisorption	70	65	4

Hydrogen can be stored by six different methods and phenomena (Züttel et al., 2003). The main hydrogen storage methods and techniques are given in Table 5.9. The characteristics of six basic hydrogen storage methods are given in Table 5.10. The major challenge with the method of oxidation of reactive metals is the reversibility and the control of the thermal reduction process in order to produce the metal in a solar furnace. Sodium and lithium have a gravimetric hydrogen density of 3 mass% and 6.3 mass%, respectively. Pressurized hydrogen gas occupies a great deal of volume compared with, for example, gasoline with equal energy content, about 30 times larger in volume at 100 bar gas pressure. Condensed hydrogen is about 10 times denser, but is much too expensive to produce and maintain (Jensen et al., 1999). There are also obvious safety concerns with the use of pressurized or liquefied hydrogen in vehicles (David, 2005). Hence, boron has an important role here.

Storing hydrogen in a carbon structure is another form of chemical bonding. New forms of carbon structures are currently being researched and promise the best and safest approach as a reversible gas absorption technology. This research is the design and use of carbon nanostructures, either nanotubes or nanofibers.

The metal hydrides provide a safe method for fuel storage in hydrogen-powered vehicles. Charging and discharging of the hydride tanks is a process that can be repeated an indefinite number of times provided that the hydride material does not become contaminated. The hydrogen would be transported from the production plant either as a gas or in liquefied form. The liquefied hydrogen, in comparison to gaseous hydrogen, offers the advantages of low pressure and low bulk, but containment difficulties arise from the cryogenic nature of the liquefied gas (Demirbas, 2002).

Thermal compression of hydrogen using reversible metal hydride alloys offers an economical alternative to traditional mechanical hydrogen compressors. The hydrogen pressure in a metal hydride increases exponentially with increasing temperature. By employing successively higher-pressure hydride alloy stages in series, high-pressure ratios can be generated. For example, a five-stage hydride compressor will compress a 1.43 atm inlet pressure to 346.94 atm resulting in a compression ratio of 242.6 (Surmen and Demirbas, 2002).

Glass microspheres can be used to safely store high-pressure hydrogen. The glass spheres are filled by being immersed in high-pressure hydrogen gas after warming to about 675 K. The fill rate is a function of glass properties, gas permeability, temperature and pressure differential. The spheres are then cooled, locking the hydrogen inside the glass balls. The subsequent increase in temperature will release the hydrogen trapped in the spheres.

In the physisorption process a gas molecule interacts with several atoms at the surface of the solid. Once a monolayer of adsorbate molecules is formed the gaseous molecule interacts with a surface of the liquid or solid adsorbate. Therefore, the binding energy of the second layer of adsorbate molecules is similar to the latent heat of sublimation or vaporization of the adsorbate.

5.6.1 Hydrogen Storage with Metal Hydrides

Metals, intermetallic compounds, and alloys generally react with hydrogen and form mainly solid metal–hydrogen compounds (MH_n). Hydrides exist as ionic, polymeric covalent, volatile covalent and metallic hydrides. Hydrogen reacts at elevated temperatures with many transition metals and their alloys to form hydrides. Many of the MH_n show large deviations from ideal stoichiometry (n = 1, 2, 3) and can exist as multiphase systems.

Using metal hydrides in electrochemical batteries is an old and rapidly improving method for hydrogen storage. Solid-state materials are attractive due to improved safety, a high energy density, and better energy efficiency (no compression or liquefaction). They are capable of absorbing and desorbing hydrogen with small pressure variations. Utilization of hydrides is also a promising technique for on-board hydrogen storage. A new method is the use of nanostructural materials such as carbon and boron nitride nanotubes, which are known to have the property to store gases within their structure (Fakioglu et al., 2004).

Table 5.11 Hydrogen contents of metal hydrides

Metal hydride	Wt.% hydrogen based on formula
$LiBH_4$	21.5
$Al(BH_4)_3$	16.8
$LiAlH_2(BH_4)_2$	15.2
$Mg(BH_4)_2$	14.8
$Ti(BH_4)_3$	13.0
$Fe(BH_4)_3$	11.9
$Ca(BH_4)_2$	11.5
$Zr(BH_4)_3$	8.8

When hydrogen combines with the metal alloy (in granular form or particles), an exothermic reaction occurs. The gas is thus stored in these metal particles until some heat is applied to release the hydrogen and build up the pressure in the tanks. When a metal hydride absorbs hydrogen, heat is given off. A hydride cold-start heater can be developed that instantly heats an automobile's catalytic converter when the car is started to dramatically reduce overall exhaust pollution up to 80%.

Hydrogen can be chemically bonded to either metal or liquid hydrides. Metal hydrides such as FeTi compounds are used to store hydrogen by bonding it to the surface of the material. As discussed later, the iron-titanium alloy acts as a sponge to absorb the hydrogen, thus becoming a metal hydride ($FeTiH_{1.6}$) with a physical appearance like that of a fine silvery powder. The safest method for hydrogen storage is the "metal hydride" system (Williamson and Edeskuty, 1986; Veziroglu, 1975). The low-temperature hydrides, $FeTiH_2$ and $LaNi_5H_7$, hold hydrogen loosely and evolve it at low temperatures. The high-temperature hydrides, MgH and Mg_2NiH_4, only release hydrogen at high temperatures since they have high binding enthalpies (Dinga, 1988).

Metal hydrides generate hydrogen gas via reversible pyrolysis reactions, i.e.,

$$2M + nH_2 \leftrightarrows 2MH_n + \text{Heat} \tag{5.48}$$

where M is a metal or an alloy. Such reactions are reversible and hydrogen can be stored by hydriding the metal under high pressure exothermically (Fakioglu et al., 2004). Table 5.11 shows the hydrogen contents of metal hydrides. Table 5.12 shows the characteristics of some metal hydrides. Theoretical reversible capacities of alanates such as $NaAlH_4$ and $LiAlH_4$ have been studied to some extent, where the maximum theoretical reversible capacity of $NaAlH_4$ is 5.5% by weight.

Hydrolysis is defined as the reaction of a hydride with water to liberate hydrogen gas. The reactions are as follows (Fakioglu et al., 2004):

$$MH_n + nH_2O \rightarrow M(OH)_n + nH_2 \tag{5.49}$$

where M is a metal and n is its valence, or,

$$MXH_4 + 4H_2O \rightarrow 4H_2 + MOH + H_3XO_3 \tag{5.50}$$

$$NaBH_4 + 2H_2O \rightarrow NaBO_2 + 4H_2 + \text{Heat} \tag{5.51}$$

There are two classes of hydrides: metallic hydrides and complex hydrides. The main difference between these two is the transition of metals to ionic or cova-

Table 5.12 Properties of some metal hydrides

Alloy	Weight (kg)	Weight of H_2 (kg)	Energy of H_2 (MJ)	Energy (MJ/kg)
Fe Ti	563	5.4	767	1.362
Ti Mn TiF	568	6.0	848	1.492
$LaNi_5$	180	2.5	353	1.962
Fe Mn Ti	433	5.0	706	1.629

lent compounds for the complex hydrides upon absorbing hydrogen. The complex hydrides of boron represent a very interesting and challenging new hydrogen storage material.

Hydrogen storage in boron hydrides is a complex process consisting of many mechanistic steps and depends on important parameters. The boron surface has to be able to dissociate the hydrogen molecule and to allow hydrogen atoms to move easily in order to be able to store hydrogen. Metals differ in the ability to dissociate hydrogen, this ability being dependent on surface structure, morphology and purity (David, 2005).

The number of hydrogen atoms per metal atom is 2 in many cases (Zhou, 2005). This kind of complex shows the highest volumetric density and the highest gravimetric density at room temperature known today in lithiumtetrahydroboride (lithiumborohydride, $LiBH_4$). $LiBH_4$ and $NaBH_4$ can reversibly absorb/desorb hydrogen at moderate temperatures, and have therefore, received much attention (Gross et al., 2002; Bogdanovic and Schwickardi, 1997; Bogdanovic et al., 2000; Zaluska et al., 2000; Zaluska et al., 1999).

Direct synthesis from the metal, boron and hydrogen at 825–975 K and 30–150 bar H_2 has yielded the lithium salt, and such a method is generally applicable to groups IA and IIA metals (Goerrig, 1958). The reaction involving either the metal or the metal hydride, or the metal together with triethylborane in an inert hydrocarbon has formed the basis of a patent.

$$M + B + 2H_2 \rightarrow MBH_4 \tag{5.52}$$

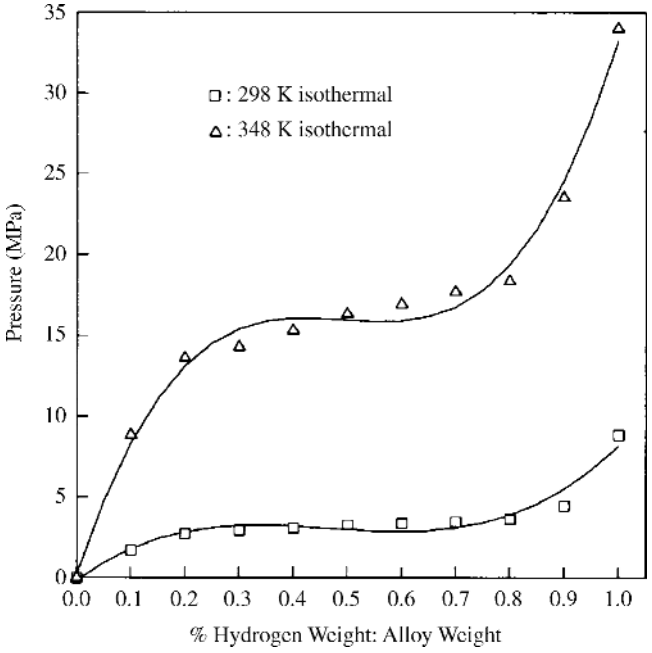

Fig. 5.7 Hydrogen absorption capacity of metal hydride alloy

M is Li, Na, K, etc., in Eq. 5.52. The decomposition of the compounds can proceed in one of the following directions:

$$MBH_4 \rightarrow M + B + 2H_2 \quad (5.53)$$

$$MBH_4 \rightarrow MH + B + 3/2H_2 \quad (5.54)$$

M is Li, Na, K, etc., for Eqs. 5.53 and 5.54.

The thermal decomposition, at least in the early stages, is reversible, as shown by the higher decomposition temperature in the presence of hydrogen than in vacuum or inert gas, and also by the existence of a rapid isotopic exchange between tetrahydroboride and deuterium at $T > 625$ K (Züttel et al., 2003).

The compound with the highest gravimetric hydrogen density at room temperature known today is $LiBH_4$. Therefore, this complex hydride could be the ideal hydrogen storage material for mobile applications. $LiBH_4$ desorbs 3 or 4 hydrogen in the compound upon melting at 553 K and decomposes into LiH and boron. The desorption process can be catalyzed by adding SiO_2 and significant thermal desorption was observed starting at 373 K (Züttel et al., 2003). Recently it has been shown, that the hydrogen desorption reaction is reversible and the end-products lithium hydride and boron absorb hydrogen at 980 K and 200 bar to form $LiBH_4$. The scientific understandings of the mechanism of the thermal hydrogen desorption from $LiBH_4$ and the absorption remains a challenge and more research work has to be carried out (Züttel et al., 2004).

Thermal compression of hydrogen using reversible metal hydride alloys offers an economical alternative to traditional mechanical hydrogen compressors. The hydrogen pressure in a metal hydride increases exponentially with increasing temperature. The hydrogen absorption capacity of a metal hydride alloy at 298 and 348 K is given in Fig. 5.7. The pressure rise generated in a single hydride heat exchanger is about 300%.

5.6.2 Hydrogen Absorption/Desorption with Oxygen-Contaminated Boron Film

The capability of H absorption decreased by 30–50% compared to the pure boron film without oxygen contamination. After the discharge, the depth profile of the oxygen atoms was not changed, which means that a stable oxide layer had formed. The reduction of the H absorption capability occurs probably because the formation of the boron oxide prevents H atoms from becoming trapped in the form of B–H bonding. Most of the retained H atoms can be released by heating up to 775 K with the oxygen contamination. The required temperature for H evacuation is slightly higher than that for the pure boron film. In addition, a small peak was observed at around 475 K. The reduction of H retention can be attributed to the oxide formation followed by the decrease of dangling bond, and thus, the decrease of H trapping sites (Tsuzuki et al., 1999).

5.6.3 Hydrogen Storage with Carbon Structures

In 1997 the journal *Nature* was the first publication to discuss the possibility of hydrogen storage in carbon material containing single-walled carbon nanotubes, which estimated for purified tubes a high possible storage capacity at room temperature and ambient pressure (Dillon et al., 1997). This article initiated tremendous research activity on the use of different nanocarbon structures for potential hydrogen storage.

Activated carbon has been extensively studied for its gas storage properties. This material was found to be ineffective for storing hydrogen, because only a small percentage of the surface strongly interacted with the hydrogen molecules at ambient temperatures and pressures (Dillon and Heben, 2001). The more recently discovered nanomaterials such as carbon nanotubes (CNTs) and graphitic nanofibers (GNFs) have renewed attention on carbon as an absorbent (Dillon et al., 1997; Fan et al., 1999; Chen et al., 1999; Gupta and Srivastava, 2000).

5.6.3.1 Carbon Nanotubes (CNTs)

Carbon nanotube technology is the other new direction being pursued in the search for high-capacity hydrogen storage media. Since their discovery in 1991 by the Japanese electron microscopist Sumio Iijima significant research has been undertaken to improve synthesis methods and more accurately characterize the unique mechanical and chemical properties of carbon nanotubes (Iijima, 1991). Nanotubes can exist as single-walled or as multiwalled units and can be pristine or doped usually with an alkali metal. As a result of van der Waals forces nanotubes can be bundled to form sites where hydrogen can be adsorbed inside the tubes. Carbon nanotubes are microscopic tubes of carbon, two nanometers (billionths of a meter) across, that store hydrogen in microscopic pores on the tubes and within the tube structures. There are a number of options for hydrogen storage in carbon nanotubes. Carbon nanotubes are fullerene-related structures, which consist of graphene microscopic cylinders closed at either end with caps containing pentagonal rings. The apparent advantage of carbon nanotubes is that they are theoretically capable of storing from about 4.2 to 6.5% of their own weight in hydrogen.

5.6.3.2 Carbon Nanofibers and Fullerenes

Another variant in carbon nanostructures is carbon nanofiber technology. Carbon nanofibers are grown by the decomposition of hydrocarbons or carbon monoxide over a metal catalyst, and the fibers comprise graphite sheets aligned in a set direction. Graphite nanofibers are ideal for selective gas absorption, as reported by Gupta and Srivastava (2000) who achieved hydrogen adsorption capacities of ~10 wt.% for GNFs grown by thermal cracking. Fan et al. (1999), observed vapor-grown car-

bon fibers exhibiting 10–13 wt.% hydrogen storage, almost twice as high as the 5.7 wt.% capacity reported by Chen et al. (1999) for the same material.

Fullerenes carbon C_{60} and C_{70} have been shown to reversibly store hydrogen. Theoretically, fullerene C_{60} can be hydrogenated up to $C_{60}H_{60}$, which corresponds to 7.7% weight of hydrogen.

5.7 Hydrogen Storage Materials

Hydrogen may be stored on board a vehicle as a gas bound with certain metals, as a liquid in cryogenic containers, or as highly compressed gas in ultrahigh-pressure (69 MPa) vessels. On-board hydrogen storage approaches presently being examined by developers include compressed hydrogen gas, cryogenic gas and liquid hydrogen, metal hydrides, high surface area adsorbents, and chemical hydrogen storage media (Ozturk and Demirbas, 2007).

The density of hydrogen in a storage material is crucial for mobile applications. Hydrogen can be stored by six different methods and phenomena (Züttel et al., 2003):

1. Liquid hydrogen in cryogenic tanks (at 21 K)
2. High-pressure gas cylinders (up to 800 bar)
3. Adsorbed hydrogen on materials with a large specific surface area (at $T < 100$ K)
4. Absorbed on interstitial sites in a host metal (at ambient pressure and temperature)
5. Oxidation of reactive metals, e.g., Li, Na, with water
6. Chemically bonded in covalent and ionic compounds (at ambient pressure)

The main challenge with storing in terms of oxidation of reactive metals is the reversibility and the control of the thermal reduction process in order to produce the metal in a solar furnace, where Na and Li have a gravimetric hydrogen density of 3 mass% and 6.3 mass%, respectively.

The density of liquid hydrogen is 70.8 kg/m³ and that of solid hydrogen is 70.6 kg/m³. But the condensation temperature of hydrogen at 1 bar is 21 K and the vaporization enthalpy at the boiling point is 452 kJ/kg. As the critical temperature of hydrogen is 32 K (above this temperature hydrogen is gaseous), liquid hydrogen containers are open systems to prevent strong overpressure. Therefore, heat transfer through the container leads directly to the loss of hydrogen. The continuously evaporated hydrogen may be catalytically burnt with air in the overpressure safety system of the container or collected again in a metal hydride (Schlapbach and Züttel, 2001).

The iron–titanium alloy, FeTi, acts as a sponge to absorb the hydrogen, thus becoming a metal hydride ($FeTiH_{1.6}$). Its physical appearance is like that of a fine silvery powder. The safest method for hydrogen storage is then this metal hydride system (Veziroglu, 1975). When hydrogen combines with the metal alloy (in granu-

lar form or particles), an exothermic reaction occurs. The gas is thus stored in these metal particles until some heat is applied to release the hydrogen and build up the pressure in the tanks. When a metal hydride absorbs hydrogen, heat is given off. This process could be used as a cold-start heater that instantly heats an vehicle's catalytic converter when the car is started, thereby dramatically reducing overall exhaust pollution up to 80%.

Thus, metal hydrides provide a safe method for storing fuel in hydrogen-powered vehicles. Charging and discharging of the hydride tanks is a process that can be repeated an indefinite number of times provided that the hydride material does not become contaminated.

5.7.1 Boron Hydrides as Metal Hydrides

As mentioned above, the safest method for hydrogen storage is the metal hydride system (Williamson and Edeskuty, 1986; Veziroglu, 1975). When hydrogen combines with the metal alloy, an exothermic reaction occurs. The gas is then stored in the metal particles until some applied heat releases the hydrogen and builds up pressure in the tanks. Heat is then emitted when a metal hydride absorbs hydrogen.

Boron absorbs hydrogen and forms hydrides. There are two classes of hydrides: metallic hydrides and complex hydrides, with the main difference being the transition of metals to ionic or covalent compounds for the complex hydrides upon absorbing hydrogen.

Boron chemistry is an interesting field of research, which includes plenty of boron hydrides. Some of which are stable, but some are unstable and interconvertible to each other, while producing hydrogen (Turker, 2001). Diborane (B_2H_6) can be synthesized via various reactions (Durant and Durant, 1970) and produce hydrogen by treatment with H_2O, NH_3, ROH, etc. (Durant and Durant, 1970; Schriver and Atkins, 1990). The molecular orbital bonding scheme for diborane has been discussed extensively (Lippard and Ucko, 1968). Tetraborane (B_4H_{10}) can be obtained by means of various synthetic routes and it also forms by the slow decomposition of diborane (Huhey, 1978; Cotton and Wilkinson, 1967):

$$2B_2H_6 \leftrightarrows B_4H_{10} + H_2 \tag{5.55}$$

B_4H_{10} decomposes from heat treatment (at 363–373 K) to produce diborane (Durant and Durant, 1970; Cotton and Wilkinson, 1967) or at elevated temperatures (at 453–473 K) to produce B_5H_{11} and B_5H_9. B_5H_{11} is known as unstable pentaborane because it decomposes in a few hours in the cold, mainly to H_2 and $B_{10}H_{14}$ (Durant and Durant, 1970).

The necessary condition for hydrogen storage is that the thermodynamic and kinetic conditions are fulfilled. In that case, a metal exposed to hydrogen gas absorbs hydrogen until equilibrium is established. There are a number of reaction steps that kinetically may hinder a hydrogen-storing system from reaching its

thermodynamical equilibrium of hydrogen storage within a reasonable time. The reaction rate of a metal-hydrogen system is therefore a function of pressure and temperature (David, 2005).

The storage of hydrogen in boron hydrides is a complex process consisting of numerous mechanistic steps, depending on many important parameters. For instance, the boron surface must be able to dissociate the hydrogen molecule and to allow hydrogen atoms to move easily in order to be able to store hydrogen. Metals differ in the ability to dissociate hydrogen, this ability being dependent on surface structure, morphology and purity (David, 2005).

5.7.2 Hydrogen in Mechanically Milled Amorphous Boron

Hydrogen can be absorbed in amorphous boron by mechanical milling under hydrogen atmosphere, the amount of which has reached up to about 2.3 mass% after 80 h of milling. The trapped hydrogen can be desorbed only as molecular hydrogen in a temperature range of 330–1000 K. Thus the hydrogen desorption in boron is achieved at relatively low temperatures with molecular hydrogen as the sole product (Wang et al., 2003). In contrast to the case of mechanically prepared nanostructured graphite, in which hydrogen desorbs at high temperatures together with desorption of hydrocarbons, hydrogen desorption in boron can be achieved at relatively low temperatures with molecular hydrogen as the sole product. The revealed hydrogenation properties, especially the attracting dehydriding aspect, warrant further investigations of the B–H system from the viewpoint of hydrogen energy storage (Wang et al., 2003).

5.7.3 Boron Complex Hydrides

In metal hydrides, the number of hydrogen atoms per metal atom is 2 in many cases (Zhou, 2005). Groups 1–3, light metals, e.g., Li, Mg, B, Al, build a large variety of metal–hydrogen complexes. They are especially interesting because of their light weight and the number of hydrogen atoms per metal atom, which in many cases is 2. The main difference between these complex hydrides and the previously described metallic hydrides is the transition to an ionic or covalent compound of the metals upon hydrogen absorption. Table 5.13 shows the physical properties of some selected complex hydrides (Züttel et al., 2003). The highest volumetric density and the highest gravimetric density at room temperature known today belong to $LiBH_4$ (18.4 mass%). $LiBH_4$ has stability compared to other chemical hydrides, and can easily be converted to H_2. As for $NaBH_4$, along with $LiBH_4$, it can reversibly absorb/desorb hydrogen at moderate temperatures and has therefore received considerable attention (Gross et al., 2002; Bogdanovic and Schwickardi, 1997; Bogdanovic et al., 2000; Zaluska et al., 2000; Zaluski et al., 1999).

Table 5.13 Physical properties of selected complex hydrides

Formula	M (g/mol)	ρ (g/cm³)	T_m (K)	T_{dec} (K)	X (mass%)	Reference
$LiBH_4$	21.784	0.66	541	653	18.4	Schlesinger and Brown, 1940
$NaBH_4$	37.83	1.074	778	673	10.6	Knacke et al., 1991
$LiAlH_4$	37.95	0.917	> 398	398	9.5	Knacke et al., 1991
KBH_4	53.94	1.178	858	773	7.4	Knacke et al., 1991
$NaAlH_4$	54.0	1.27	451	483	7.4	Bogdanovic and Schwickardi, 1997
Mg_2NiH_4	111.3	2.72		553	3.6	Sandrock and Thomas, 2001
Mg_2FeH_6	110.5	2.72		593	5.4	Yvon, 1998
Mg_3MnH_7	134.9	2.30		553	5.2	Yvon, 1998
$BaReH_9$	332.5	4.86		< 373	2.7	Yvon, 1998

M molecular mass, ρ gravimetric density, T_m melting point, T_{dec} decomposition temperature, X gravimetric hydrogen density

Boron builds a large variety of metal-hydrogen complexes. It is especially interesting because of its light weight and the number of hydrogen atoms per metal atom. The hydrogen in the complex hydrides is often located at the corners of a tetrahedron with boron in the center. The negative charge of the anion, $[BH_4^-]$, is compensated by a cation, e.g., Li or Na. The hydride complexes of borane and the tetrahydroborates $M(BH_4)$ are interesting storage materials (M = Li, Na, K, etc.); however, they are known to be stable and decompose only at elevated temperatures and often above the melting point of the complex (Züttel et al., 2004).

Schlesinger and Brown synthesized the lithiumtetrahydroboride (lithiumborohydride) ($LiBH_4$) by the reaction of ethyllithium with diborane (B_2H_6) in 1940 (Schlesinger and Brown, 1940). It was the first report of a pure alkali metal tetrahydroboride. The direct reaction of the corresponding metal with diborane in ethereal solvents under suitable conditions produces high yields of the tetrahydroborides (Huhey, 1978):

$$2MH + B_2H_6 \leftrightarrows 2MBH_4 \tag{5.56}$$

where M is a metal such as Li, Na, K, etc.

Stasinevich and Egorenko (1968) investigated the alkali metal tetrahydroborides by means of thermal analysis in hydrogen at pressures up to 10 bar. The thermal decomposition, at least in the early stages, is reversible, as is shown by the decomposition temperature being higher in the presence of hydrogen than in vacuum or inert gas (Ostroff and Sanderson, 1957; Mesmer and Jolly, 1962) and also by the existence (Mesmer and Jolly, 1962; Brown et al., 1952) of a rapid isotopic exchange between tetrahydroboride and deuterium at $T > 625$ K (Züttel et al., 2003).

The compound with the highest gravimetric hydrogen density at room temperature known today is $LiBH_4$ (~18 mass%). Therefore, this complex hydride could be the ideal hydrogen storage material for mobile applications. $LiBH_4$ desorbs 3 or 4 hydrogen in the compound upon melting at 553 K and decomposes into LiH and B. The process of desorption can be catalyzed by adding SiO_2; significant thermal desorption was observed starting at 373 K (Züttel et al., 2003). Recently it has been shown that the hydrogen desorption reaction is reversible and the end-products lithium hydride and boron absorb hydrogen at 963 K and 200 bar to form $LiBH_4$. The scientific understanding of the mechanism of the thermal hydrogen desorption from $LiBH_4$ and the absorption remains a challenge; thus, more work must be carried out (Züttel et al., 2004). $LiBH_4$ desorbs the hydrogen only at temperatures from 353 K up to 873 K (Brown et al., 1952). The decomposition temperature of $NaAlH_4$ can be lowered by doping the hydride with TiO_2, and the reversibility of the reaction for several desorption/absorption cycles is shown. This is a good example demonstrating the potential of boron hydrides.

$Al(BH_4)_3$ is a complex hydride with a very high gravimetric hydrogen density of 17 mass%, and the highest known volumetric hydrogen density of 150 kg/m³. $Al(BH_4)_3$ has a melting point of 208 K and is the only liquid hydride at room temperature. The complex hydrides of boron represent a very interesting and challenging new hydrogen storage material.

5.8 Hydrogen Fuel for Internal Combustion Engine

Water is a readily available resource for generating of hydrogen. With 70% of the world's surface being covered by water, it is one of the most abundant resources on this planet. For more than a decade, hydrogen as an alternative to traditional energy sources such as oil and natural gas has been the focus of research and development efforts in all technologically advanced countries of the world. In the pursuit for a cleaner world, hydrogen power is perhaps the cleanest fuel alternative.

Hydrogen exhibits the highest heating value of all chemical fuels (Demirbas, 1998). The energy from 1 kg hydrogen is equivalent to 2.1 kg natural gas and 2.8 kg petroleum. A hydrogen engine has both the advantages of the high thermal efficiency of a diesel engine (Das, 1996) and the excellent operating performance of a petrol engine (Gren and Glasson, 1992). In the automotive world, hydrogen can be utilized in two ways: hydrogen can be internally combusted to generate power or it can be combined with oxygen in a fuel cell to generate electricity.

Internal combustion engines that run on hydrogen are virtually identical to their gasoline predecessors. The difference is that water is the byproduct from combustion with oxygen rather than harmful pollutants. Because the engine runs on hydrogen gas, there are some slight changes in the engine design. Hydrogen has a very wide explosive range (from 4 to 75% in air) in which it can be combined with oxygen to explode. This explosive range is significantly larger than that of gasoline. Therefore, on hydrogen internal combustion engines (HICEs) there is an electronic

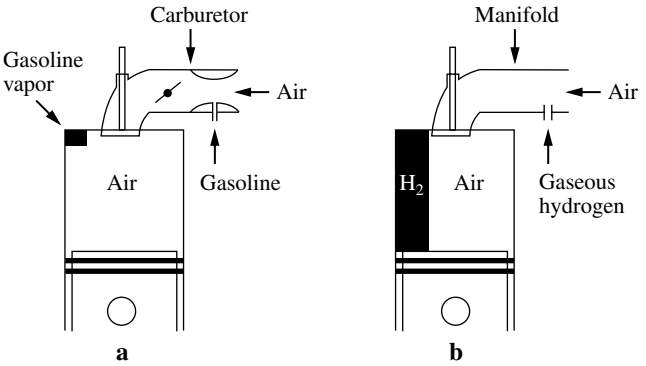

Fig. 5.8 **a** Carburetor in a liquid gasoline-fueled Otto engine. **b** Manifold in gaseous hydrogen-fueled modified engine systems

throttle system which controls the air coming into the engine so that the engine can always run at a lean mixture of air and fuel. Another characteristic of HICEs is that they use high-compression pistons such that more power can be achieved from the combustion process.

The performance of hydrogen fuel cell vehicles must be comparable or superior to today's gasoline vehicles in order to achieve widespread commercial success. The most critical issues facing the automotive fuel cell developer are overall power plant efficiency, interfacing the power plant with the fuel's infrastructure, achieving ultralow or zero emissions, and power plant costs. Fuel cells are very useful as power sources in remote locations, such as spacecraft, remote weather stations, large parks, rural locations, and in certain military applications. There are numerous prototype or production cars and buses based on fuel cell technology being researched or manufactured. A practical commercial fuel cell automobile is not expected until at least 2015 according to the automobile industry.

The hydrogen would be transported from the production plant either as a gas or in liquefied form. The liquefied hydrogen, in comparison to gaseous hydrogen, offers the advantages of low pressure and low bulk, but containment difficulties arise from the cryogenic nature of the liquefied gas (Demirbas, 2002). Figure 5.8a,b shows a carburetor in a liquid gasoline-fueled Otto engine and the manifold in a gaseous hydrogen-fueled modified engine system.

5.8.1 Advantages of Hydrogen as an Engine Fuel

Hydrogen can be used as a motor fuel, whereas neither nuclear nor solar energy can be used directly. Nuclear power requires heavy shielding to keep the neutrons away from people, but is too heavy for cars. It can be used in ships especially submarines

and aircraft carriers. Hydrogen fuel is hydrogen gas with small amounts of oxygen and other materials added. Benefits include cleaner air, cleaner water, and better health. Hydrogen is also a renewable resource.

Hydrogen has many properties that make it ideal as a fuel for internal combustion engines in automobiles. When hydrogen is burned in air the main product is water. Should greenhouse warming turn out to be an important problem, the key advantage of hydrogen is that carbon dioxide (CO_2) is not produced when hydrogen is burned. Hydrogen combustion does not produce toxic products such as hydrocarbons (C_xH_y), carbon monoxide (CO), oxides of sulfur (SO_x), organic acids, and CO_2. Acid rain and the CO_2 greenhouse effect could effectively be eliminated.

Hydrogen contains 2.75 times as much energy as the same weight of gasoline. Hydrogen has a high flame speed, wide flammability limits, and a high detonation temperature with lean burning, which give improved engine efficiency.

Hydrogen is a gas at 20.13 K; therefore, there is no problem in starting an engine at the coldest winter temperatures, i.e., instant start-up.

As with any gasoline engine, efficiency depends on driving conditions. At freeway speeds the hydrogen engine has demonstrated at least a 20% increase in efficiency. Hydrogen engines demonstrate the efficient operations of a diesel and the high rpm characteristics of a gasoline motor.

The thermodynamic cycle for hydrogen is much closer to the ideal Otto cycle than for either a gasoline or a diesel engine. In addition, the compression ratio can be higher.

5.8.2 Disadvantages of Hydrogen as an Engine Fuel

The main disadvantages of using hydrogen as a fuel for automobiles are huge onboard storage tanks, which are required because of hydrogen's extremely low density. Hydrogen may be stored on board a vehicle as compressed gas in ultrahigh-pressure vessels, as a liquid in cryogenic containers, or as a gas bound with certain metals in metal hydrides. It is expensive to bring hydrogen to mass production. The easiest and cheapest way to refine hydrogen is by electrolysis, which uses electricity to process hydrogen from water. However, most of our cheap electricity comes from fossil fuels, which pollute the environment.

Hydrogen can be used as a fuel directly in an internal combustion engine not much different from the engines used with gasoline. The problem is that while hydrogen supplies three times the energy per pound of gasoline, it has only one-tenth the density when the hydrogen is in a liquid form and much less when it is stored as a compressed gas. This means that hydrogen fuel tanks must be large.

Demonstrations of hydrogen-powered vehicles have usually used compressed hydrogen gas. However, because of the low density, compressed hydrogen will not give a car as useful a range as gasoline. It may be even worse than using lead-acid batteries. Hydrogen can achieve a reasonable density adsorbed in metal hydrides, but then the weight of the metals makes the system very heavy.

Hydrogen does not occur freely in nature in useful quantities. It has to be made, usually by splitting water to get the hydrogen. This requires all the energy you are going to get from burning the hydrogen and a bit more on account of inefficiencies. Therefore, hydrogen is an energy transfer medium rather than a primary source of energy.

Hydrogen is the lightest of the elements with an atomic weight of 1.0. Liquid hydrogen has a density of 0.07 grams per cubic centimeter, whereas water has a density of 1.0 g/ml and gasoline about 0.75 g/ml. A hydrogen fuel tank will have three times the size of a gasoline tank. Also it must be insulated, and this will add to its bulk. This seems entirely bearable. These facts give hydrogen both advantages and disadvantages. The advantage is that it stores approximately 2.6 times the energy per unit mass as gasoline, and the disadvantage is that it needs about four times the volume for a given amount of energy. A 15-gallon automobile gasoline tank contains 90 pounds of gasoline. The corresponding hydrogen tank would be 60 gallons, but the hydrogen would weigh only 34 pounds.

Liquid hydrogen is cold enough to freeze air, and accidents have occurred from pressure build-up following plugged valves. Limited accident experience suggests that the danger is somewhat less with hydrogen than with gasoline, because the hydrogen dissipates rapidly. Although, the release of hydrogen into a confined space like a garage risks an explosion.

5.9 Liquefaction and Compression of Hydrogen

The liquefaction of hydrogen above 20 K is not possible with known non-catalytic methods. The advantage of liquid hydrogen is its high energy mass ratio, three times that of gasoline, but up to 40% of the energy content in the hydrogen can be lost during the liquefaction operation.

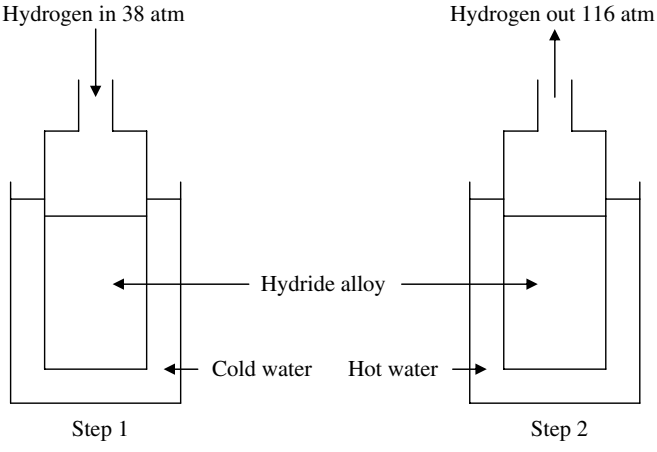

Fig. 5.9 Thermal hydrogen compression with a two-step process

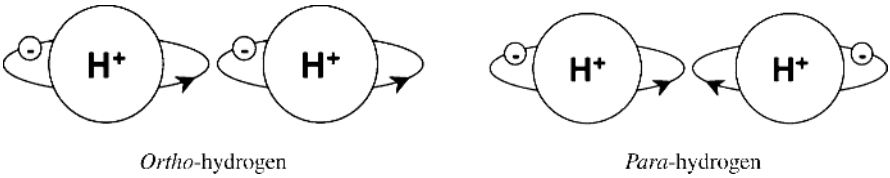

Fig. 5.10 *Ortho*- and *para*-hydrogen structures

Energy is needed to compress gases. The compression work depends on the thermodynamic compression process. The ideal isothermal compression cannot be realized. Even more energy is needed to compact hydrogen by liquefaction. Low density and extremely low boiling point of hydrogen increases the energy cost of compression or liquefaction.

The activated hydrogen molecules can be attracted to each other more than normal hydrogen molecules in the reaction medium and these attractions may result easily in liquefaction of hydrogen in reaction conditions (Fig. 5.12).

Thermal hydrogen compression with a two-step process is given in Fig. 5.9. By employing successively higher-pressure hydride alloy stages in series, high-pressure ratios can be generated. For example, a five-stage hydride compressor will compress a 0.14 MPa inlet pressure to 35 MPa, resulting in a compression ratio of 25 MPa (Surmen and Demirbas, 2002).

A major concern in liquid hydrogen storage is minimizing hydrogen losses from liquid boil-off. Because liquid hydrogen is stored as a cryogenic liquid that is at its boiling point, any heat transfer to the liquid causes some hydrogen to evaporate. Liquefaction by the Linde cycle, for example, consumes nearly 30% of the total energy contained in the hydrogen and in addition requires expensive equipment and energy to retain hydrogen in the liquid state. Up to 40% of the energy content in the hydrogen can be lost during liquefaction operation. Figure 5.10 shows the *ortho*- and *para*-structures of hydrogen. Normal hydrogen includes 75% *ortho*- and 25% *para*-hydrogen, while liquid hydrogen is composed of 0.2% *ortho*- and 99.8% *para*-structures. The source of this heat can be *ortho*-to-*para* conversion, mixing or pumping energy, radiant heating, convection heating or conduction heating. The liquid hydrogen storage is very expensive in comparison to other methods.

5.9.1 Nanocatalytic Liquefaction of Hydrogen

The experiments of nanocatalytic liquefaction of hydrogen were carried out using a platinum-supported carbon nanolayer. In the experiments, H_2PtCl_6, $6H_2O$ or H_2PtCl_6 was used as a Pt precursor. To prepare the Pt catalytic reaction nanolayer, the required amounts of H_2PtCl_6 were mixed with 5 wt.% carbon prepared by burning naphthalene in air (Demirbas, 2008).

All the runs were performed in a 100-ml cylindrical autoclave. The catalyzed carbon and hydrogen gas was loaded into an autoclave. The autoclave was cooled

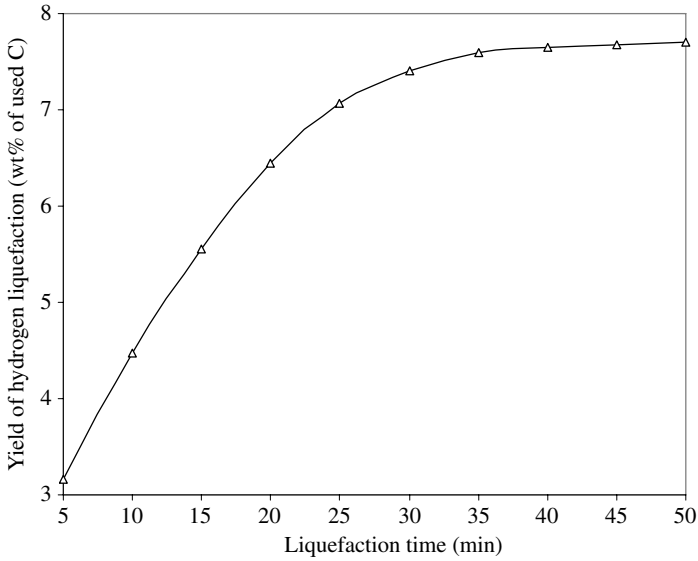

Fig. 5.11 Plot for yield of hydrogen liquefaction on Pt-supported carbon versus time

using an external liquid nitrogen bath. The nominal reaction time is 30 min. After each run, non-liquefied hydrogen gas was vented and then the autoclave was heated with an external heater for determining the liquefaction hydrogen in the reaction conditions (Demirbas, 2008).

Figure 5.11 shows the plot for yield of hydrogen liquefaction on Pt-supported carbon versus liquefaction time. The yield of hydrogen liquefaction increased with increasing liquefaction time. The nominal liquefaction time was 30 min in reaction conditions. The yield of liquefied hydrogen was 7.4% weight of Pt-catalyzed carbon.

Hydrogen consists of a mixture of two types of molecule, *ortho*-hydrogen, in which the two proton spins are parallel, and *para*-hydrogen, in which they are antiparallel. There are a number of possible methods for measuring the proportion of *ortho*- to *para*-molecules in a sample of hydrogen gas (Farkas, 1935; Stewart and Squires, 1955; Silvera and Pravica, 1998).

At hydrogen's boiling point of 20 K, the equilibrium concentration is almost all *para*-hydrogen, but at room temperature or higher, the equilibrium concentration is 25% *para*-hydrogen and 75% *ortho*-hydrogen (Noganow, 1992). The uncatalyzed conversion from *ortho*- to *para*-hydrogen proceeds very slowly, so without a catalyzed conversion step, the hydrogen may be liquefied, but may still contain significant quantities of *ortho*-hydrogen. This *ortho*-hydrogen will eventually be converted into the *para*-form in an exothermic reaction (Timmerhaus and Flynn, 1989).

Figure 5.12 shows the structure of the activated hydrogen molecule. The Pt catalyst may cause the increase of activation of the hydrogen molecule. As mentioned before, since the activated hydrogen molecules are more likely to be attracted each other than normal hydrogen molecules in the reaction medium, these attractions may result in liquefaction of hydrogen.

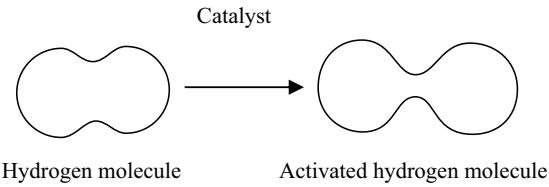

Fig. 5.12 Structure of activated hydrogen molecule

Table 5.14 Catalysts prepared from different precursors

Precursor (wt.%)	Catalyst	Composition	Loading ratio
$H_2PtCl_6 \cdot 6H_2O$	Pt	Single	5.0
$RuCl_3 \cdot 3H_2O + H_2PtCl_6 \cdot 6H_2O$	Ru	Composite	2.5
	Pt		2.5
K_2PtCl_4	Pt	Single	5.0
$RuCl_3 \cdot 3H_2O + K_2PtCl_4$	Ru	Composite	2.5
	Pt		2.5

Carbon-supported platinum (Pt) and platinum–ruthenium (Pt–Ru) alloy are one of the most popular electrocatalysts in polymer electrolyte fuel cells (PEFC). Pt supported on electrically conducting carbons, preferably carbon black, is being increasingly used as an electrocatalyst in fuel cell applications (Parker et al., 2004). Carbon-supported Pt could be prepared at loadings as high as 70 wt.% without a noticeable increase of particle size. Unsupported and carbon-supported nanoparticle Pt–Ru_{adatom} (Pt–Ru_{ad}) catalysts prepared using the surface reductive deposition technique were evaluated as anode catalysts in liquid feed PEM-DMFCs. It was found that the surface composition of unsupported Pt–Ru_{ad} nanoparticles has a significant influence on their activities as anode catalysts in direct methanol fuel cells (Cao and Bergens, 2004). Carbon-supported Pt–Ru_{ad} catalysts display higher mass activities than unsupported Pt–Ru_{ad}. The electrochemical deposition of Pt–Ru nanoparticles on carbon nanotube electrodes and their electrocatalytic properties have been investigated by He et al. (2004). Table 5.14 shows the catalysts Pt and Ru, prepared from various precursors serving as electrolytic electrodes in the fuel cells (Chaurasia et al., 2003).

Activated carbon has been extensively studied for its gas storage properties. This material was found to be ineffective for storing hydrogen, because only a small percentage of the surface strongly interacted with the hydrogen molecules at ambient temperatures and pressures (Dillon and Heben, 2001). The more recently discovered nanomaterials such as carbon nanotubes (CNTs) and graphitic nanofibers (GNFs) have renewed attention on carbon as an absorbent (Dillon et al., 1997; Fan et al., 1999; Chen et al., 1999; Gupta and Srivastava, 2000).

Another technology being pursued in the search for high-capacity hydrogen storage media is that of carbon nanotubes. Since their discovery in 1991 by Sumio

Iijima, significant research has been undertaken to improve synthesis methods and more accurately characterize the unique mechanical and chemical properties of carbon nanotubes (Iijima, 1991). Nanotubes can exist as single-walled or as multi-walled units and can be pristine or doped usually with an alkali metal. As a result of van der Waals forces nanotubes can be bundled to form sites where hydrogen can be adsorbed inside the tubes. Carbon nanotubes are microscopic tubes of carbon, two nanometers (billionths of a meter) across, that store hydrogen in microscopic pores on the tubes and within the tube structures. There are a number of options for hydrogen storage in carbon nanotubes. Carbon nanotubes are fullerene-related structures, which consist of graphene microscopic cylinders closed at either end with caps containing pentagonal rings. The apparent advantage of carbon nanotubes is that they are theoretically capable of storing from about 4.2 to 6.5% of their own weight in hydrogen.

Carbon nanofiber technology is another variant in carbon nanostructures. Carbon nanofibers are grown by the decomposition of hydrocarbons or carbon monoxide over a metal catalyst, and the fibers comprise graphite sheets aligned in a set direction. Graphite nanofibers are ideal for selective gas absorption, with results reported by Gupta and Srivastava (2000) who achieved hydrogen adsorption capacities of ~10 wt.% for GNFs grown by thermal cracking. Fan et al. (1999) observed vapor-grown carbon fibers exhibiting 10–13 wt.% hydrogen storage, almost twice as high as the 5.7 wt.% capacity reported by Chen et al. (1999) for the same material.

Summary

Hydrogen energy is a promising alternative solution because it is clean and environmentally safe. It also produces negligible levels of greenhouse gases and other pollutants when compared with the fossil fuel energy sources they replace.

Hydrogen can be obtained by direct electrolysis, by direct thermal conversion, thermochemically, photochemically, photoelectrochemically, and biochemically from water.

There are a few different approaches for hydrogen transportation and storage. Hydrogen can be stored as a compressed gas (up to 800 bar), as a liquid (at 21 K) and in solid-state compounds. The first two methods are well-established technologies with several limitations, the most important of which is their energy-intensive character. Conventional storage systems consist of classical high-pressure tanks and insulated liquid hydrogen systems. Compressing hydrogen is similar to compressing natural gas, though as hydrogen is less dense the compressors need very high-quality seals. The main disadvantages of using hydrogen as a fuel for automobiles are huge on-board storage tanks, which are required because of hydrogen's extremely low density. Hydrogen may be stored on board a vehicle as compressed gas in ultrahigh-pressure vessels, as a liquid in cryogenic containers, or as a gas bound with certain metals in metal hydrides.

References

Abe, T., Suzuki, E., Nagoshi, K., Miyashita, K., Kaneko, M. 1999. Electron source in photoinduced hydrogen production on Pt-supported TiO_2 particles. J Phys Chem B 103:1119–1123.

Adesina, A.A., Meeyoo, V., Foulds, G. 1995. Thermolysis of hydrogen sulphide in an open tubular reactor. Int J Hydrogen Energy 20:777–783.

Al-Shamma, L., Naman, S.A. 1989. Kinetic study for thermal production of hydrogen from H_2S by heterogeneous catalysis of vanadium sulfide in a flow system. Int J Hydrogen Energy 14:173–179.

Amiridis, M.D., Duevel, R.V., Wachs, I.E. 1999. The effect of metal oxide additives on the activity of V_2O_5/TiO_2 catalysts for the selective catalytic reduction of nitric oxide by ammonia. Appl Catal B Environ 20:111–122.

Anderson, C., Bard, A.J. 1995. Improved photocatalyst of TiO_2/SiO_2 prepared by a sol-gel synthesis. J Phys Chem 99:9882–9885.

Arakawa, H., Sayama, K. 2000. Solar hydrogen production: significant effect of Na_2CO_3 addition on water splitting using simple oxide semiconductor photocatalysts. Catal Surv Jpn 4:75–80.

Arni, S. 2004. Hydrogen-rich gas production from biomass via thermochemical pathways. Energy Edu Sci Technol 13:47–54.

Arpe, H. (Ed.) 1989 Ullmann's Encyclopedia of industrial chemistry. Hydrogen sulfide. 5th edn. Vol. A13, VCH, Weinheim, pp. 467–485.

Asahi, R., Morikawa, T., Ohwaki, T., Aoki, K., Tao, Y. 2001. Visible-light photocatalysis in nitrogen-doped titanium oxides. Science 293:269–271.

Ashokkumar, M., Kudo, A., Saito, N., Sakata, T. 1994. Semiconductor sensitization by RuS_2 colloids on TiO_2 electrodes. Chem Phys Lett 229:383–388.

Ashokkumar, M., Maruthamuthu, P. 1989. Factors influencing the photocatalytic efficiency of WO_3 particles. J Photochem Photobiol A 49:249–258.

Bak, T., Nowotny, J., Rekas, M., Sorrell, C.C. 2002. Photoelectrochemical hydrogen generation from water using solar energy: materials-related aspects. Int J Hydrogen Energy 27:991–1022.

Balat, M., Ozdemir, N. 2005. New and renewable hydrogen production processes. Energy Sources 27:1285–1298.

Bamwenda, G.R., Arakawa, H. 2000. Cerium dioxide as a photocatalyst for water decomposition to O-2 in the presence of Ce-aq(4+) and Fe-aq(3+) species. J Mol Catal A 161:105–113.

Baykara, S.Z., Ayfer Kale, A., Veziroglu, T.N. 2005. Possibilities for hydrogen production from H_2S in Black Sea. Proceedings International Hydrogen Energy Congress and Exhibition IHEC 2005, Istanbul, Turkey, 13–15 July 2005.

Baykara, S.Z., Figen, E.H., Kale, A., Veziroglu, T.N. 2007. Hydrogen from hydrogen sulphide in Black Sea. Int J Hydrogen Energy 32:1246–1250.

Berry, G.D., Pasternak, A.D., Rambach, G.D., Smith, J.R., Schock, R.N. 1996. Hydrogen as a future transportation fuel. Energy 21:289–303.

Bessekhouad, Y., Trari, M. 2002. Photocatalytic hydrogen production from suspension of spinel powders AMn_2O_4 (A=Cu and Zn). Int J Hydrogen Energy 27:357–362.

Bhaumik, A., Inagaki, S. 2001. Mesoporous titanium phosphate molecular sieves with ion-exchange capacity J Am Chem Soc 123:691–696.

Bishara, A., Salman, O.A., Khraishi, N., Marafi, A. 1987. Thermochemical decomposition of hydrogen sulfide by solar energy. Int J Hydrogen Energy 12:679–685.

Bogdanovic, B., Brand, R.A., Marjanovic, A., Schwikardi, M., Tolle, J. 2000. Metal doped sodium aluminum hydrides as potential new hydrogen storage materials. J Alloys Comp 302:36–58.

Bogdanovic, B., Schwickardi, M. 1997. Ti-doped alkali metal aluminum hydrides as potential novel reversible hydrogen storage materials. J Alloys Comp 253–254:1–9.

Borgarello, E., Kiwi, J., Graetzel, M., Pelizzetti, E., Visca, M. 1982. Visible-light induced water cleavage in colloidal solutions of chromium-doped titanium-dioxide particles. J Am Chem Soc 104:2996–3002.

Brown, W.G., Kaplan, L., Wilzbach, K.E. 1952. The exchange of hydrogen gas with lithium and sodium borohydrides. J Am Chem Soc 74:1348.

Buhler, N., Meier, K., Reber, J.F. 1984. Photochemical hydrogen-production with cadmium sulfide suspensions. J Phys Chem 88:3261–3268.

Buntkowsky, G., Walaszek, B., Adamczyk, A., Xu, Y., Limbach, H.-H., Chaudret, B. 2006. Mechanism of nuclear spin initiated para-H_2 to ortho-H_2 Conversion. Phys Chem Chem Phys 16:1929–1935.

Caglar, A., Ozmen, H. 2000. Hydrogen: as an attractive fuel in future. Energy Edu Sci Technol 6:1–18

Cao, D., Bergens, S.H. 2004. Pt–Ru_{adatom} nanoparticles as anode catalysts for direct methanol fuel cells. J Power Sources 134:170–180.

Cerveramarch, S.C., Borrell, L., Gimenez, J., Simarro, R., Andujar, J.M. 1992. Solar hydrogen photoproduction from sulfide sulfite substrate. Int J Hydrogen Energy 17:683–688.

Chaurasia, P.B.L., Ando, Y., Tanaka, T. 2003. Regenerative fuel cell with chemical reactions. Energy Convers Manage 44:611–628.

Chen, P., Wu, X., Lin, J., Tan, K.L. 1999. High H_2 uptake by alkali-doped carbon nanotubes under ambient pressure and moderate temperatures. Science 285:91–93.

Choi, W., Termin, A., Hoffmann, M. 1994. The role of metal ion dopants in quantum-sized TiO_2. J Phys Chem 98:13669–13679.

Choudhary, T.V., Goodman, D.W. 1999. Stepwise methane steam reforming: a route to CO-free hydrogen. Catal Lett 59:93–94.

Choudhary, T.V., Goodman, D.W. 2000. CO-free production of hydrogen via stepwise steam reforming of methane. J Catal 192:316–321.

Clark, P.D., Dowling, N.I., Hyne, J.B., Moon, D.L. 1995. Production of hydrogen and sulfur from hydrogen sulfide in refineries and gas processing plants. Alberta Sulphur Res Quart Bull 32:11–28.

Cotton, F.A., Wilkinson, G. 1967. Advanced Inorganic Chemistry. Interscience, New York.

Dagan, G., Tomkiewicz, M. 1994. Preparation and characterization of TiO_2 aerogels for use as photocatalysts. J NonCryst Sol 175:294–302.

Das, L.M. 1996. Hydrogen–oxygen reaction mechanism and its implication to hydrogen engine combustion. Int J Hydrogen Energy 21:703–715.

David, E. 2005. An overview of advanced materials for hydrogen storage. J Materials Proc Technol 162–163:169–177.

De, G.C., Roy, A.M., Bhattacharya, S.S. 1996. Effect of n-Si on the photocatalytic production of hydrogen by Pt-loaded CdS and CdS/ZnS catalyst. Int J Hydrogen Energy 21:19–23.

Demirbas, A. 1998. Determination of combustion heat of fuels by using non-calorimetric experimental data. Energy Edu Sci Technol 1:7–12.

Demirbas, A. 2002. Fuel properties of hydrogen, liquefied petroleum gas (LPG), and compressed natural gas (CNG) for transportation. Energy Sources 24:601–610.

Demirbas, A. 2007. Storage and transportation opportunities of hydrogen. Energy Sources Part B 2:287–295.

Demirbas, A. 2008. Nano-catalytic liquefaction of hydrogen. Energy Sources Part A 30:1540–1547.

Desilvestro, J., Neumannspallart, M. 1985. Photoredox reactions on semiconductors at open circuit reduction of Fe^{3+} on WO_3 electrodes and particle suspensions. J Phys Chem 89:3684–3689.

Dillon, A.C., Heben, M.J. 2001. Hydrogen storage using carbon adsorbents: past, present and future. Appl Phys A 72:133–142.

Dillon, A.C., Jones, K.M., Bekkedahl, T.A., Kiang, C.H., Bethune, D.S., Heben, M.J. 1997. Storage of hydrogen in single-walled carbon nanotubes. Nature 386:377–378.

Dinga, G.P. 1988. Hydrogen: The ultimate fuel and energy carrier. J Chem Educ 65:688–691.

Domen, K., Kudo, A., Onishi, T. 1986. Mechanism of photocatalytic decomposition of water into H-2 and O-2 over NiO – $SrTiO_3$. J Catal 102:92–98.

Domen, K., Naito, S., Onishi, T., Tamaru, K. 1982. Photocatalytic decomposition of liquid water on a NiO–$SrTiO_3$ catalyst. Chem Phys Lett 92:433–434.

Durant, P.J., Durant, B. 1970. Introduction to advanced inorganic chemistry. Longman, London.

Fakioglu, E., Yurum, Y., Veziroglu, T.N. 2004. A review of hydrogen storage systems based on boron and its compounds. Int J Hydrogen Energy 29:1371–1376.
Fan, Y.-Y., Liao, B., Liu, M., Wei, Y.-L. Liu, M.-Q., Cheng, H.-M. 1999. Hydrogen uptake in vapor grown carbon nanofibers. Carbon 37:1649–1652.
Faherburch, A.L., Bube, R.H. 1983. Fundamentals of Solar Cells. Academic, New York.
Farkas, A. 1935. Orthohydrogen, parahydrogen and heavy hydrogen. Cambridge University Press, Cambridge.
Fletcher, E.A., Noring, J.E., Murray, J.P. 1984. Hydrogen-sulfide as a source of hydrogen. Int Hydrogen Energy 9:587–593.
Fonash, S.J. 1981. Solar cells device physics. Academic, New York.
Fujishima, A., Honda, K. 1972. Electrochemical photolysis of water at a semiconductor electrode. Nature 238:37–38.
Fujishima, A., Rao, T.N., Tryk, D.A. 2000. Titanium dioxide photocatalysis. J Photochem Photobiol C Photochem Rev 1:1–21.
Galinska, A., Walendziewski, J. 2005. Photocatalytic water splitting over Pt TiO_2 in the presence of sacrificial reagents. Energy Fuels 19:1143–1147.
Goerrig, D. 1958. DBP German Patent 1,077,644.
Green, M.A. 1982. Solar cells. Prentice-Hall, Englewood Cliffs, NJ.
Gringue, D., Horowitz, G., Garnier, E. 1987. Stabilization of CdS and CdSe photoelectrodes modified by a catalyst-containing polythiophene coating. Ber Buns Phys Chem 91:402–405.
Gross, K.J., Thomass, G.J., Jensen, C.M. 2002. Catalyzed alanates for hydrogen storage. J Alloys Comp 330–332:683–690.
Gupta, B.K., Srivastava, O.N. 2000. Synthesis and hydrogenation behaviour of graphitic nanofibres. Int J Hydrogen Energy 25:825–830.
Gurunathan, K. 2000. Photobiocatalytic production of hydrogen using sensitized TiO–MV^{2+} system coupled *Rhodopseudomonas* capsulate. J Mol Catalysis A Chem 156:59–67.
Gurunathan, K., Maruthamuthu, P. 1995. Photogeneration of hydrogen using visible-light with undoped doped alpha-Fe_2O_3 in the presence of methyl viologen. Int J Hydrogen Energy 20:287–295.
Gurunathan, K., Maruthamuth, P., Sastri, M.V.C. 1997. Photocatalytic hydrogen production by dye-sensitized Pt/SnO_2 and Pt/SnO_2/RuO_2 in aqueous methyl viologen solution. Int J Hydrogen Energy 22:57–62.
Hacisalihoglu, B., Demirbas, A.H., Hacisalihoglu, S. 2008. Hydrogen from gas hydrate and hydrogen sulfide in the Black Sea. Energy Edu Sci Technol 21:109–115.
He, P., Gu, G., Shao, L., Zhang, Y. 2000. Research on low temperature thermo-chemical conversion to oil process from sewage sludge. Water Sci Tech 42:301–308.
He, Z., Chen, J., Liu, D., Zhou, H., Kuang, Y. 2004. Electrodeposition of Pt–Ru nanoparticles on carbon nanotubes and their electrocatalytic properties for methanol electrooxidation. Diamond Related Mater 13:1764–1770.
Herrmann, J.M., Disdier, J., Pichat, P. 1986. Photoassisted platinum deposition on TiO_2 powder using various platinum complexes. J Phys Chem 90:6028–6034.
Hitoki, G., Takata, T., Kondo, J., Hara, M., Kobayashi, H., Domen, K. 2002. An oxynitride, TaON, as an efficient water oxidation photocatalyst under visible light irradiation (lambda $\lambda \leq 500$ nm). Chem Commun 16:1698–1699.
Hohhmann, P. 2002. Tomorrow's energy: hydroen, fuel cells, and the prospects for a cleaner planet. MIT Press, Cambridge, MA, London, UK, 2002.
Höhlein, B., von Andrian, S., Grube, Th., Menzer, R. 2000. Critical assessment of power trains with fuel-cell systems and different fuels. J Power Sources 86:243–249.
Huang, C., Raissi, T.-A. 2005. Analysis of sulfur–iodine thermochemical cycle for solar hydrogen production. Part I: decomposition of sulfuric acid. Solar Energy 78:632–646.
Huhey, E.J. 1978. Inorganic chemistry. Harper and Row, New York.
Hwang, D.W., Kim, H.G., Jang, J.S., Bae, S.W., Ji, S.M., Lee, J.S. 2004. Photocatalytic decomposition of water–methanol solution over metal-doped layered perovskites under visible light irradiation. Catal Today 93–5:845–850.

Hwang, D.W., Kim, J., Park, T.J., Lee, J.S. 2002. Mg-doped WO_3 as a novel photocatalyst for visible light-induced water splitting. Catal Lett 80:53–57.

Iijima, S. 1991. Helical microtubules of graphitic carbon. Nature 354:56–57.

Inoue, Y., Kubokawa, T., Sato, K. 1991. Photocatalytic activity of alkali-metal titanates combined with Ru in the decomposition of water. J Phys Chem 95:4059–4063.

Ishihara, T., Nishiguchi, H., Fukamachi, K., Takita, Y. 1999. Effects of acceptor doping to $KTaO_3$ on photocatalytic decomposition of pure H_2O. J Phys Chem B 103:1–3.

Ishikawa, A., Takata, T., Kondo, J.N., Hara, M., Kobayashi, H., Domen, K. 2002. Oxysulfide $Sm_2Ti_2S_2O_5$ as a stable photocatalyst for water oxidation and reduction under visible light irradiation (lambda $\lambda \leq 650$ nm). J Am Chem Soc 124:13547–13553.

Jang, J.S., Kim, H.G., Reddy, V.R., Bae, S.W., Ji, S.M., Lee, J.S. 2005. Photocatalytic water splitting over iron oxide nanoparticles intercalated in $HTiNb(Ta)O_5$ layered compounds. J Catal 231:213–222.

Jensen, C.M., Zidan, R., Mariels, N., Hee, A., Hagen, C. 1999. Advanced titanium doping of sodium aluminum hydride: segue to a practical hydrogen storage material? Int J Hydrogen Energy 24:461–465.

Kamat, P.V. 1989. Photoelectrochemistry in particulate systems 9. Photosensitized reduction in a colloidal TiO_2 system using anthracene-9-carboxylic acid as the sensitizer. J Phys Chem 93: 859–864.

Kamat, P.V., Fox, M.A. 1983. Photo-sensitization of TiO_2 colloids by Erythrosin-B in acetonitrile. Chem Phys Lett 102:379–384.

Kapoor, M.P., Inagaki, S., Yoshida, H. 2005. Novel zirconium-titanium phosphates mesoporous materials for hydrogen production by photoinduced water splitting. J Phys Chem B 109:9231–9238.

Kato, H., Kudo, A. 1998. New tantalite photocatalysts for water decomposition into H_2 and O_2. Chem Phys Lett 295:487–492.

Kato, H., Kudo, A. 1999a. Photocatalytic decomposition of pure water into H_2 and O_2 over$SrTa_2O_6$ prepared by a flux method. Chem Lett 11:1207–1208.

Kato, H., Kudo, A. 1999b. Highly efficient decomposition of pure water into H_2 and O_2 over $NaTaO_3$ photocatalysts. Catal Lett 58:153–155.

Kawai, T., Sakata, T. 1980. Photocatalytic hydrogen production from liquid methanol and water. J Chem Soc Chem Commun 15:694–695.

Kennedy, I.H., Dunnwald, D. 1983. Photooxidation of organic-compounds at doped alpha Fe_2O_3 electrodes. J Electrochem Soc 130:2013–2016.

Kennedy, L.A., Fridman, A.A., Saveliev, A.V. 1995. Superadiabatic combustion in porous media: wave propagation, instabilities, new type of chemical reactor. Fluid Mechanics Res 22:1–25.

Khan, S.U.M., Al-Shahry, M., Ingler, W.B. 2002. Efficient photochemical water splitting by a chemically modified n-TiO_2. Science 297:2243–2245.

Kida, T., Guan, G., Yoshida, A. 2003. $LaMnO_3$/CdS nanocomposite: a new photocatalyst for hydrogen production from water under visible light irradiation. Chem Phys Lett 371:563–567.

Kida, T., Guan, G., Yamada, N., Ma, T., Kimura, K., Yoshida, A. 2004. Hydrogen production from sewage sludge solubilized in hot-compressed water using photocatalyst under light irradiation. Int J Hydrogen Energy 29:269–274.

Kiuchi, H., Nakamura, T., Funaki, K., Tanaka, T. 1982. Recovery of hydrogen from hydrogen sulfide with metals and metal sulfides. Int J Hydrogen Energy 7:477–482.

Kiwi, J., Morrison, C. 1984. Heterogeneous photocatalysis-dynamics of charge-transfer in lithium-doped anatase-based catalyst powders with enhanced water photocleavage under ultraviolet-irradiation. J Phys Chem 88:6146–6152.

Knacke, O., Kubaschewski, O., Hesselmann, K. 1991. Thermochemical Properties of Inorganic Substances, 2nd edn. Springer, Berlin Heidelberg New York.

Koca, A., Sahin, M. 2002. Photocatalytic hydrogen production by direct sun light from sulfide/sulfite solution. Int J Hydrogen Energy 27:363–367.

Koca, A., Sahin, M. 2003. Photocatalytic hydrogen production by direct sunlight: a laboratory experiment. J Chem Edu 80:1314–1315.

Kohno, M., Kaneko, T., Ogura, S., Sato, K., Inoue, Y. 1998. Dispersion of ruthenium oxide on barium titanates ($Ba_6Ti_{17}O_{40}$, $Ba_4Ti_{13}O_{30}$, $BaTi_4O_9$ and $Ba_2Ti_9O_{20}$) and photocatalytic activity for water decomposition. J Chem Soc Faraday Trans 94:89–94.

Kormann, C., Bahnemann, D.W., Hoffmann, M.R. 1988. Preparation and characterization of quantum-size titanium-dioxide. J Phys Chem 92:5196–5201.

Koroneos, C., Dompros, A., Roumbas, G., Moussiopoulos, N. 2005. Advantages of the use of hydrogen fuel as compared to kerosene. Res Conser Recyc 44:99–113.

Kotera, Y., Todo, N., Fukuda, K. 1976. Process for production of hydrogen and sulfur from hydrogen sulfide as raw material. US Patent No. 3,962,409.

Kudo, A. 2001. Development of photocatalyst materials for water splitting with the aim at photon energy conversion. J Ceram Soc Jpn 109:81–88.

Kudo, A., Tanaka, A., Domen, K., Maruya, K., Aika, K., Onishi, T. 1988. Photocatalytic decomposition of water over $NiO–K_4Nb_6O_{17}$ catalyst. J Catal 111:67–76.

Kudo, A., Kato, H., Nakagawa, S. 2000. Water splitting into H_2 and O_2 on new $Sr_2M_2O_7$ (M = Nb and Ta) photocatalysts with layered perovskite structures: factors affecting the photocatalytic activity. J Phys Chem B 104:571–575.

Lee, J., Kato, T., Fujishima, A., Honda, K. 1984. Photoelectrochemical oxidation of alcohols on polycrystalline zinc-oxide. Bull Chem Soc Jpn 57:1179–1183.

Linsebigler, A., Lu, G., Yates, J.T. 1995. Co-chemisorption on TiO_2-oxygen vacancy site influence on co-adsorption. J Chem Phys 103:9438–9443.

Lippard, S.J., Ucko, D.A. 1968. Transition metal borohydride complexes. II. Th reaction of copper(I) compounds with boron hydride anions. Inorg Chem 7:1051–1058.

Litter, M.I. 1999. Heterogeneous photocatalysis: transition metal ions in photocatalytic systems. Appl Catal B Environ 23:89–114.

Luinstra, E. 1996. Hydrogen from H_2S: a review of the leading processes. Proceedings of 7th GRI Sulfur Recovery Conference, Gas Research Institute, Chicago, pp. 149–165.

Mackor, A., Blasse, G. 1981. Visible-light induced photocurrents in $SrTiO_3$-$LaCrO_3$ single crystalline electrodes. Chem Phys Lett 77:6–8.

Malinowska, B., Walendziewski, J., Robert, D., Weber, J.V., Stolarski, M. 2003a. Titania aerogels: preparation and photocatalytic tests. Int J Photoenergy 5:147–152.

Malinowska, B., Walendziewski, J., Robert, D., Weber, J.V., Stolarski, M. 2003b. The study of photocatalytic activities of titania and titania-silica aerogels. Appl Catal B Environ 46:441–451.

Maruthamuthu, P., Ashokkumar, M. 1988. Hydrogen generation using $Cu(II)/WO_3$ and oxalic acid by visible-light. Int J Hydrogen Energy 13:677–680.

Maruthamuthu, P., Ashokkumar, M., Gurunathan, K., Subramanian, E., Sastri, M.V.C. 1989. Hydrogen evolution from water with visible radiation in presence of $Cu(II)/WO_3$ and electron relay. Int J Hydrogen Energy 14:525–528.

Maruthamuthu, P., Gurunathan, K., Subramanian, E., Sastri, M.V.C. 1993. Visible-light induced hydrogen-production with $Cu(II)/Bi_2O_3$ and Pt/ Bi_2O_3/RuO_2 from aqueous methyl viologen solution. Int J Hydrogen Energy 18:9–13.

Maruthamuthu, P., Muthu, S., Gurunathan, K.,Ashokkumar, M., Sastri, M.V.C. 1992. Photobiocatalysis: hydrogen evolution using a semiconductor coupled with photosynthetic bacteria. Int J Hydrogen Energy 17:863–866.

Megalofonos, S.K., Papayannakos, N.G. 1997. Kinetics of catalytic reaction of methane and hydrogen sulphide over MoS2. J Appl Catal A General 165:249–258.

Mesmer, R.E., Jolly, W.L. 1962. The exchange of deuterium with solid potassium hydroborate. J Am Chem Soc 84:2039–2042.

Midilli, A., Olgun, H., Ayhan, T. 2000. Solar hydrogen production from hazelnut shells. Int J Hydrogen Energy 25:723–732.

Midilli, A., Dogru, M., Akay, G., Howarth, C.R. 2002. Hydrogen production from sewage sludge via a fixed bed gasifier product gas. Int J Hydrogen Energy 27:1035–1041.

Midilli, A., Ay, M., Dincer, I., Rosen, M.A. 2005. On hydrogen and hydrogen energy strategies I: current status and needs. Renew Sust Energy Rev 9:255–271.

Miller, E., Rocheleau, R., Khan, S. 2004. A hybrid multijunction photoelectrode for hydrogen production fabricated with amorphous silicon/germanium and iron oxide thin films. Int J Hydrogen Energy 29:907–914.

Miranda, R. 2004. Hydrogen from lignocellulosic biomass via thermochemical processes. Energy Edu Sci Technol 13:21–30.

Moon, J., Takagi, H., Fujishiro, Y., Awano, M. 2001. Preparation and characterization of the Sb doped TiO_2 photocatalysts. J Mater Sci 36:949–955.

Moon, S.C., Mametsuka, H., Tabata, S., Suziki, E. 2000. Photocatalytic production of hydrogen from water using TiO_2 and B/TiO_2. Catal Today 58:125–132.

Namon, S.A., Aliwi, S.M., Alemara, K. 1986. Hydrogen-production from the splitting of H_2S by visible-light irradiation of vanadium sulfides dispersion loaded with RuO_2. Int J Hydrogen Energy 11:33–38.

Navvio, J.A., Testa, J.J., Djedjeian, P., Padron, J.R., Rodriguez, D., Litter, M.I. 1999. Iron-doped titania powders prepared by a sol-gel method. Appl Catal A General 178:191–203.

Ni, M., Leung, K.H.M., Leung, D.Y.C., Sumathy, K. 2007. A review and recent developments in photocatalytic water-splitting using TiO_2 for hydrogen production. Renew Sustain Energy Rev 11:401–425.

Ni, M., Leung, K.H.M., Sumathy, K., Leung, D.Y.C. 2004. Water electrolysis: a bridge between renewable resources and hydrogen. Proceedings of the International Hydrogen Energy Forum, Beijing, PRC, pp. 475–480.

Nikandrov, V.V., Shlyk, M.A., Zorin, N.A., Gogotov, I.N., Krosnovsky, A.A. 1988. Efficient photoinduced electron-transfer from inorganic semiconductor TiO_2 to bacterial hydrogenase. Febs Lett 234:111–114.

Nishikawa, T., Nakajima, T., Shinohara, Y. 2001. An exploratory study on effect of the isomorphic replacement of TiO_2. J Mol Struct Theochem 545:67–74.

Noganow, L.S. 1992. Hydrogen. McGraw-Hill Encyclopedia of Science & Technology, 7th edn. Vol. 8. McGraw-Hill, New York, pp. 581–588.

Ogura, S., Kohno, M., Sato, K., Inoue, Y. 1997. Photocatalytic activity for water decomposition of RuO_2-combined $M_2Ti_6O_{13}$ (M = Na, K, Rb, Cs). Appl Surf Sci 121:521–524.

Ohno, T., Saito, S., Fujihara, K., Matsumura, M. 1996. Photocatalyzed production of hydrogen and iodine from aqueous solutions of iodide using platinum-loaded TiO_2 powder. Bull Chem Soc Jpn 69:3059–3064.

Okamoto, K., Yamamoto, Y., Tanaka, H., Itaya, A. 1985. Kinetics of heterogeneous photocatalytic decomposition of phenol over anatase TiO_2 powder. Bull Chem Soc Jpn 58:2023–2028.

Oosawa, Y. 1984. Photocatalytic decomposition of aqueous hydroxylamine solution over anatase and precious metal anatase. J Phys Chem 88:3069–3074.

Ostroff, A., Sanderson, R. 1957. Oxidation and thermal decomposition of sodium and potassium borohydrides. J Inorg Nuclear Chem 4:230–231.

Ozturk, T., Demirbas, A. 2007. Boron compounds as hydrogen storage materials. Energy Sources Part A 29:1415–1423.

Parker, S.F., Taylor, J.W., Albers, P., Lopez, M., Sextl, G., Lennon, D., McInroy, A.R., Sutherland, I.W. 2004. Inelastic neutron scattering studies of hydrogen on fuel cell catalysts. Vibration Spectrosc 35:179–182.

Petrov, K. 1995. The Black Sea and hydrogen energy. Int J Hydrogen Energy 16:805–808.

Plass, J.H., Barbir, F., Miller, H.P., Veziroglu, T.N. 1990. Economics of hydrogen as a fuel for surface transportation. Int J Hydrogen Energy 15:663–668.

Piotrowska, A., Walendziewski, J. 2005. Photocatalytic hydrogen production from the water over titania aerogels under UV irradiation. Proceedings International Hydrogen Energy Congress and Exhibition IHEC 2005, Istanbul, Turkey.

Ranjit, K.T., Cohen, H., Willner, I., Bossmann, S., Braun, A. 1999. Lanthanide oxide-doped titanium dioxide: effective photocatalysts for the degradation of organic pollutants. J Mater Sci 34:5273–5280.

Reber, J.F., Meier, K. 1984. Photochemical production of hydrogen with zinc-sulfide suspensions. J Phys Chem 88:5903–5913.

Rifkin, J. 2002. The hydrogen economy. Jeremy P. Tarcher/Penguin, New York.

Rocheleau, R.E., Vierthaler, M. 1994. Optimization of multijunction a-Si:H solar cells using an integrated optical/electrical model, *in* Proceedings of the 21st World Conference on Photovoltaic Energy Conversion, pp. 567–570. Institute for Electrical and Electronics Engineers, Honolulu, HI.

Rostrup-Nielsen, J.R. 1984. Catalytic steam reforming, *in* Catalysis: science and technology, Vol. 5, J.R. Anderson, M. Boudart. Springer, Berlin Heidelberg New York, pp. 1–117.

Sandrock, G., Thomas, G. 2001.The IEA/DOE/SNL on-line hydride databases. Appl Phys A Mater Sci Proc 72A:153–155.

Sato, J., Saito, N., Nishiyama, H., Inoue, Y. 2001. New photocatalyst group for water decomposition of RuO_2-loaded p-block metal (In, Sn, and Sb) oxides with d^{10}configuration. J Phys Chem B 105:6061–6063.

Sayama, K. Arakawa, H. 1992a. Significant effect of carbonate addition on stoichiometric photodecomposition of liquid water into hydrogen and oxygen from platinum titanium (IV) oxide suspension. J Chem Soc Chem Commun 2:150–152.

Sayama, K., Arakawa, H. 1992b. Remarkable effect of Na_2CO_3 addition on photodecomposition of liquid water into H_2 and O_2 from suspension of semiconductor powder loaded with various metals. Chem Lett 2:253–256.

Sayama, K., Arakawa, H. 1996. Effect of carbonate addition on the photocatalytic decomposition of liquid water over a ZrO_2 catalyst. J Photochem Photobiol A Chem 94:67–68.

Sayama, K., Arakawa, H. 1993. Photocatalytic decomposition of water and photocatalytic reduction of carbon-dioxide over ZrO_2 catalyst. J Phys Chem 97:531–533.

Sayama, K., Arakawa, H. 1994. Effect of Na_2CO_3 addition on photocatalytic decomposition of liquid water over various semiconductor catalysts. J Photochem Photobiol A Chem 77:243–247.

Schlapbach, L., Züttel, A. 2001. Hydrogen-storage materials for mobile applications. Nature 414:353–358.

Schlesinger, H.J., Brown, H.C., 1940. Metallo borohydrides. III. Lithium borohydride. J Am Chem Soc 62:3429–3435.

Schriver, D.F., Atkins, P.W. 1990. Langford CH. Inorganic Chemistry. ELBS, Oxford.

Serban, A., Nissenbaum, A. 2000. Light induced production of hydrogen from water by catalysis with ruthenium melanoidins. Int J Hydrogen Energy 25:733–737.

Serpone, N., Borgarello, E., Gratzel, M. 1984. Visible-light induced generation of hydrogen from H_2S in mixed semiconductor dispersions: improved efficiency through inter-particle electron transfer. Chem Commun 6:342–344.

Shahbazov, J., Usupov, I. 1994. Non-trading sources of energy for hydrogen. Int J Hydrogen Energy 19:863–864.

Silvera, I.F., Pravica, M.G. 1998. Hydrogen at megabar pressures and the importance of ortho–para concentration. J Phys Condens Matter 10:11169–11177.

Slimane, R.B., Lau, F.S., Dihu, R., Bingue, J.P., Saveliev, A.V., Fridman, A.A., Kennedy, L.A. 2002. Production of hydrogen by superadiabatic decomposition of hydrogen sulfide, 14th World Hydrogen Energy Conference, Montreal, Quebec, Canada, 9–14 June 2002.

Slimane, R.B., Lau, F.S., Khinkis, M., Bingue, J.P., Saveliev, A.V., Kennedy, L.A. 2004a. Conversion of hydrogen sulfide to hydrogen by superadiabatic partial oxidation: thermodynamic consideration. Int J Hydrogen Energy 29:1471–1477.

So, W.W., Kim, K.J., Moon, S.J. 2004. Photo-production of hydrogen over the CdS–TiO_2 nanocomposite particulate films treated with $TiCl_4$. Int J Hydrogen Energy 29:229–234.

Stasinevich, D.S., Egorenko, G.A. 1968. A thermographic investigation of sodium hydroborate-sodium hydride system. Russ J Inorg Chem 133:341–343.

Stewart, A.T., Squires, G.L. 1955. Analysis of ortho- and para-hydrogen mixtures by the thermal conductivity method. J Sci Instrum 32:26–29.

Stolarek, P., Ledakowicz, S. 2001. Thermal processing of sewage sludge by drying, pyrolysis, gasification and combustion. Water Sci Tech 44:333–339.

Surmen, Y., Demirbas, A. 2002. Thermochemical conversion of residual biomass to hydrogen for Turkey. Energy Sources 24:403–411.

Suzuki, A., Nakamura, T., Yokoyama, S. 1990. Effect of operating parameters on thermochemical liquefaction of sewage sludge. J Chem Eng Jpn 23:6–11.
Suzuki, A., Nakamura, T., Yokoyama, S., Ogi, T., Koguchi, K. 1988. Conversion of sewage sludge to heavy oil by direct thermochemical liquefaction. J Chem Eng Jpn 21:288–293.
Takata, T., Shinohara, K., Tanaka, A., Hara, M., Kondo, J.N., Domen, K. 1997a. A highly active photocatalyst for overall water splitting with a hydrated layered perovskite structure. J Photochem Photobiol A: Chem 106:45–49.
Takata, T., Furumi, Y., Shinohara, K., Tanaka, A., Hara, M., Kondo, J.N., Domen, K. 1997b. Photocatalytic decomposition of water on spontaneously hydrated layered perovskites. Chem Mater 9:1063–1064.
Talavera, R.R., Vargas, S., Arroyo-Murillo, R., Montiel-Campos, R., Haro-Poniatowski, E. 1997. Modification of the phase transition temperatures in titania doped with various cations. J Mater Res 12:439–443.
Timmerhaus, C., Flynn, T.M. 1989. Cryogenic engineering. Plenum, New York.
Tryk, D.A., Fujishima, A., Honda, K. 2000. Recent topics in photoelectrochemistry: achievements and future prospects. Electrochim Acta 45:2363–2376.
Tsuzuki, K., Eiki, H., Inoue, N., Sagara, A., Noda, N., Hirohata, Y., Hino; T. 1999. Hydrogen absorption/desorption behavior with oxygen contaminated boron film. J Nuclear Mat 266–269:247–250.
Turker, L. 2001. Diborane–tetraborane conversion in C60 vesicles-a theoretical study. Int J Hydrogen Energy 26:837–842.
Urban, D.L., Antal, M.J. 1982. Study of the kinetics of sewage pyrolysis using DSC and DTA. Fuel 61:799–806.
Veziroglu, T. 1975. Hydrogen Energy, Part B. Plenum, New York.
Viswanathan, B. 2006. An introduction to energy sources. Indian Institute of Technology, Madras, India.
Wang, H. 2007. Hydrogen production from a chemical cycle of H_2S splitting. Int J Hydrogen Energy 32:3907–3914.
Wang, P., Orimo, S., Tanabe, K., Fujii, H. 2003. Hydrogen in mechanically milled amorphous boron. J Alloys Comp 350:218–221.
Williamson, K., Edeskuty, F. 1986. Recent developments in hydrogen technology, Vol. I–II. CRC, Boca Raton, FL.
Wu, J., Uchida, S., Fujishiro, Y., Yin, S., Sato, T. 1999a. Synthesis and photocatalytic properties of $HTaWO_6$/(Pt, TiO_2) and $HTaWO_6$/(Pt, Fe_2O_3) nanocomposites. Int J Inorg Mater 1:253–258.
Wu, J., Uchida, S., Fujishiro, Y., Yin, S., Sato, T. 1999b. Synthesis and photocatalytic properties of $HNbWO_6$/TiO_2 and $HNbWO_6$/Fe_2O_3 nanocomposites. J Photochem Photobiol A Chem 128:129–133.
Wu, J., Yin, S., Lin, Y., Lin, J.M., Huang, M.L., Sato, T. 2001. Hydrothermal synthesis of $HNbWO_6$/MO series nanocomposites and their photocatalytic properties. J Mat Sci 36:3055–3059.
Yokoyama, S., Suzuki, A., Murakami, M., Ogi, T., Koguchi, K., Nakamura, E. 1987. Liquid fuel production from sewage sludge by catalytic conversion using sodiumcarbonate. Fuel 66:1150–1155.
Yoshimura, J., Ebina, Y., Kondo, J., Domen, K., Tanaka, A. 1993. Visible-light induced photocatalytic behavior of a layered perovskite type niobate. J Phys Chem B 97:1970–1973.
Yvon, K. 1998. Complex transition-metal hydrides. Chimia 52:613–619.
Zaluska, A., Zaluski, L., Strom-Oslen, J.O. 2000. Sodium alanates for reversible hydrogen storage. J Alloys Comp 298:125–134.
Zaluski, L., Zaluska, A., Strom-Olsen, J.O. 1999. Hydrogenation properties of complex alkali metal hydrides fabricated by mechano-chemical synthesis. J Alloys Comp 290:71–78.
Zaman, J., Chakma, A. 1995. Production of hydrogen and sulphur from hydrogen sulphide. Fuel Proc Technol 41:159–198.
Zhou, L. 2005. Progress and problems in hydrogen storage methods. Renew Sustain Energy Rev 9:395–408.
Zou, Z.G., Ye, J.H., Sayama, K., Arakawa, H. 2001. Direct splitting of water under visible light irradiation with an oxide semiconductor photocatalyst. Nature 424:624–627.

Züttel, A., Wenger, P., Rentsch, S., Sudan, P., Maurona, P., Emmenegger, C. 2003. $LiBH_4$ a new hydrogen storage material. J Power Sources 118:1–7.
Züttel, A., Wenger, P., Sudan, P., Maurona, P., Orimo, S. 2004. Hydrogen density in nanostructured carbon, metals and complex materials. Mater Sci Eng B 108:9–18.